

The smoothed finite element method (S-FEM): A framework for the design of numerical models for desired solutions

Gui-Rong Liu*

Department of Aerospace Engineering and Engineering Mechanics, University of Cincinnati, Cincinnati 45219, USA

**Corresponding author: E-mail: liugr@uc.edu*

© Higher Education Press and Springer-Verlag GmbH Germany, part of Springer Nature 2019

ABSTRACT The smoothed finite element method (S-FEM) was originated by G R Liu by combining some meshfree techniques with the well-established standard finite element method (FEM). It has a family of models carefully designed with innovative types of smoothing domains. These models are found having a number of important and theoretically profound properties. This article first provides a concise and easy-to-follow presentation of key formulations used in the S-FEM. A number of important properties and unique features of S-FEM models are discussed in detail, including 1) theoretically proven softening effects; 2) upper-bound solutions; 3) accurate solutions and higher convergence rates; 4) insensitivity to mesh distortion; 5) Jacobian-free; 6) volumetric-locking-free; and most importantly 7) working well with triangular and tetrahedral meshes that can be automatically generated. The S-FEM is thus ideal for automation in computations and adaptive analyses, and hence has profound impact on AI-assisted modeling and simulation. Most importantly, one can now purposely design an S-FEM model to obtain solutions with special properties as wish, meaning that S-FEM offers a framework for design numerical models with desired properties. This novel concept of numerical model on-demand may drastically change the landscape of modeling and simulation. Future directions of research are also provided.

KEYWORDS computational method, finite element method, smoothed finite element method, strain smoothing technique, smoothing domain, weakened weak form, solid mechanics, softening effect, upper bound solution

1 Introduction

1.1 Brief history on the finite element method (FEM)

As one of the most successful numerical methods, the FEM [1–4] has been well developed and now widely applied to solve mechanics problems in sciences and engineering, including structural analysis and design, material design and evaluation, fluid flows, thermodynamics, soil mechanics, biomechanics, electromagnetism, just to name a few. The key ideas and techniques of the FEM were mainly established, fine-tuned and perfected over 1950s–1980s. The democratization and popularization of FEM are largely supported by three important factors: solid mathematic theory, fast development of computer hard-

ware, and development of user-friendly commercial software packages. Despite the huge success, the standard FEM, however, has also some limitations, including Refs. [5,6]:

1) Poor accuracy in stresses when a linear triangular (2D) or tetrahedral (3D) mesh, or T-mesh, is used. This is due to the overly-stiff behavior rooted at the fully-compatible element-confined Galerkin weak formulation using assumed displacement field. The T-mesh is, however, the simplest and the only mesh type that can be generated automatically for complicated geometries of solids and structures. Hence, it is indispensable mesh to use in practice. Efforts to make T-mesh usable effectively are thus extremely important, and much of the efforts on meshfree methods are with this goal [7,202–204].

2) The standard FEM demands for high quality mesh, when quadrilateral (Q4) and hexahedral (H8) elements are

used. This often leads to time-consuming and costly manual operations by the analysts. In addition, sophisticated software packages are needed in the creation and checking the quality of the meshes.

3) Mapping is a must in the FEM to ensure the compatibility on the interfaces of Q4 and H8 elements. This not only leads to higher computational costs for the evaluations of the Jacobin matrix, but also poor solutions and even breakdown during computation when an element is heavily distorted. This is because the Jacobin matrix can become badly conditioned. For this reason, the analysts need to be properly trained in using a sophisticated pre-processor for creating FEM models.

4) The fully compatible FEM solution is always a lower bound (for force-driving problems, in strain energy measure). Lacking of upper bound leads to difficulty to quantify the solution errors, and to determine the necessary mesh density. Trial-and-error is often required.

5) Volumetric locking phenomenon: The solution error increases significantly for incompressible solids whose Poisson's ratio closes to 0.5, at which the bulk modulus approaches to infinite and thus dominates the strain energy of the entire system, leading to erroneous solution that is "locked" in volumetric behavior.

Alternative theory and techniques are needed to address the above-mentioned problems, a reliable numerical method that works effectively with the most simplicial T-mesh can be critically valuable.

1.2 Brief history on the smoothed finite element method (S-FEM)

The S-FEM [8–36] was originated by G R Liu and coworkers based on finite element mesh by applying the strain smoothing techniques [37] that was used to stabilize the nodal integrated Galerkin meshfree methods, and the concept of point interpolation method (PIM) used to construct meshfree shape functions [5]. The first paper of S-FEM was published in 2005 [9] using smoothing cells created based on nodes, but it was termed as LC-PIM as a part of efforts on meshfree method development using PIM. When linear PIM is used, the LC-PIM is actually the NS-FEM using linear 3-noded triangular (Tr3) elements. In 2008, the 3D version of NS-FEM (was still termed as LC-PIM) using 4-noded tetrahedral (Te4) elements was developed [10]. In 2008, the important upper-bound-solution and volumetric-lock-free properties of NS-FEM was discovered and examined in detail [11]. Since then a family of models have been established through a number of innovative constructions of smoothing domains (SDs). The S-FEM becomes a valuable combination of the standard FEM [4] with the strain smoothing operation [37] using innovative types of SDs [8] and PIM used in the meshfree techniques [5]. This novel combination effectively addresses almost all the limitations in the FEM. Typical S-FEM models developed so far are:

1) Cell-based S-FEM (CS-FEM) for both 2D and 3D problems [12,15,46,165,169,171,174,177,182,193]. The first CS-FEM paper was published in 2007 [12];

2) Node-based S-FEM (NS-FEM) for both 2D and 3D problems [20,41,99,166,176,194]. The first paper on NS-FEM was published in 2005 [9];

3) Edge-based S-FEM (ES-FEM) for 2D and 3D [21–24,33,47,61,62,72,75,77,82,88,110,129,141,172,192,197,210]. The first paper on ES-FEM was published in 2009 [21];

4) Face-based S-FEM (FS-FEM) for 3D [27–29,94,164,195]. The first paper on FS-FEM was published in 2009 [27];

5) Hybrid types of smoothing domains was also designed, in constitutive-matrix based selective manner [16,29,32–35,48–56,74,76,157,187], and in domain-based manner: S-FEM/FM-BEM [188], sub-domain S-FEM [189], ES-XFEM [85,89], α FEM [18,25,26,48,49,168,178], β FEM [36,198], etc..

Studies have found that each S-FEM model can have different properties or unique features, depending on the types of smoothing domains used [8]. These S-FEM models have already been applied to a wide class of mechanics problems of solids and structures, including:

1) Stress analysis and design for structures [8,13,163,186];

2) Vibration and dynamic analysis of various types of structures [14,47,48,67,71,72,100–108,166,176–178,206];

3) Hyperelasticity and biomechanics [35,56,156–162,187];

4) Elastic-plastic analyses [23,57,205];

5) Visco-elastoplastic analysis [24,28];

6) Contact analyses [50,51,58,59,165];

7) Heat transfer and thermo-mechanical problems [128–140,169];

8) Plates and shells [19,54,61–71,172,173];

9) Composites [68,70,72–74];

10) Structural or vibro-acoustics [109–124];

11) Limit and shakedown analyses [75,76,185];

12) Fracture mechanics, crack propagation, and fatigue [31,32,34,77–97,174];

13) Crystal plasticity modeling [36,60];

14) Stochastic analyses [98,99];

15) Impact problems [125];

16) Piezoelectricity and photonic devices [141–146];

17) Fluid-structure interactions [30,147–155];

18) Adaptive analyses [51,76,90,126,127];

19) Fluid dynamics [171] [175];

20) Porous media [182];

21) Topology optimization [142,143,184].

A detailed review on these models and their applications of S-FEM are referred to a recent review article [167]. Theoretical studies on stability and convergence for S-FEM can be found in [180,181,183]. Works on code development of S-FEM are available at [5,8,38,163,

170,179,181,190]. Some basic codes of S-FEM are available for free download at GRLab’s website: <http://www.ase.uc.edu/~liugr>.

The formulation of S-FEM can be viewed as a typical weakened weak (W^2) formulation that were used for various types of problems [38–45,200]. The W^2 formulation consists of two layers of “weakening” treatments: one for the system equation in which the displacements are approximated and used in a Galerkin weakform, and another for the strain approximation based the assumed displacements via strain smoothing and using the Gauss divergence theorem. The former make the model stiffer known stiffing effects [4], and the later makes the model softer known as the softening effects [44,45]. Because the strain approximation uses only the assumed displacements and the geometric information of the smoothing domain boundary, no addition degrees of freedom (DoFs) are introduced. These two complimentary stiffing and softening effects enable the S-FEM a number of unique features listed as follows:

1) S-FEM models are theoretically proven softer than the FEM counterparts using the same mesh [5,8]. They are found often producing more accurate solutions, higher convergence rates, and much less sensitive to mesh distortion. If the S-FEM model is a stiffer model (such as the ES-FEM and FS-FEM), the solution is always more accurate than the FEM counterpart.

2) The NS-FEM is a softer model, and offers an efficient and practical means to produce upper boundary solutions [9–11]. Together with the lower bound solution of FEM, one can now bound the solutions from both sides, which is important for solution error quantification.

3) Combining the soft effects of NS-FEM and stiff effects of FEM in the formulation stage, one can create models (such as the α FEM) that can produce “close-to-exact” solutions [18,25,109,168,178].

4) S-FEM models work exceptionally well with Triangular (2D) or Tetrahedral (3D) mesh, or T-mesh, that can be automatically generated. This is because of the use of W^2 formulation [38,40]. They are thus ideal for automation in computations and adaptive analyses, and hence has profound impact on AI-assisted modeling and simulation. In addition, S-FEM uses also polygonal elements of arbitrary shape.

5) The NS-FEM is found naturally “volumetric-locking-free” [11,195,196], which is important for simulation nonlinear problems of soft materials, such as bio-tissues.

6) The S-FEM can be viewed as a typical case of W^2 model, and hence only the shape function values are needed in the formulation, and no derivatives of the shape functions are required. Therefore, no mapping (and hence no Jacobian matrix is involved) is needed in S-FEM. This Jacobian-free feature leads to insensitivity to mesh distortion, which is important for large deformation nonlinear problems.

7) Most importantly, one can in fact purposely design an

S-FEM model to obtain solutions with special properties. The S-FEM is a framework that enable the design of models for solutions with desired properties and unique features. This novel concept of numerical model on-demand may drastically change the landscape of modeling and simulation.

2 S-FEM formulations

2.1 Strain smoothing

Consider a problem of solid mechanics defined in problem domain Ω and bounded by Γ . The problem is first divided into a set of elements to form a mesh often in the similar manner as in the standard FEM. Because the S-FEM uses smoothed strains, one needs to create smoothing domains on top of the element mesh. The problem domain is thus divided further into a set of non-overlapping and non-gap smoothing domains $\Omega_k^s (k = 1, 2, \dots, N_s)$ bounded by Γ_k^s , such that $\Omega = \bigcup_{k=1}^{N_s} \Omega_k^s$ and $\Omega_i^s \cap \Omega_j^s = \emptyset$ for $i \neq j$, where N_s is the number of the smoothing domains. The smoothed strain can then obtained for point \mathbf{x}_C in a smoothed domain using

$$\begin{aligned} \bar{\boldsymbol{\epsilon}}_k(\mathbf{x}_C) &= \int_{\Omega_k^s} \underbrace{\boldsymbol{\epsilon}^h(\mathbf{x})}_{\text{compatible strains}} \underbrace{W_k(\mathbf{x} - \mathbf{x}_C)}_{\text{weight function}} d\Omega \\ &= \int_{\Omega_k^s} \underbrace{\mathbf{L}_d \mathbf{u}^h(\mathbf{x})}_{\boldsymbol{\epsilon}^h(\mathbf{x})} W_k(\mathbf{x} - \mathbf{x}_C) d\Omega, \end{aligned} \quad (1)$$

where $\boldsymbol{\epsilon}^h(\mathbf{x})$ is the compatible strain obtained using the assumed displacements by differentiation, and \mathbf{L}_d is a matrix of differential operators. It is given as follows, respectively, for 1D, 2D, and 3D problems.

$$\mathbf{L}_d = \frac{\partial}{\partial x} \text{ for 1D, } \mathbf{L}_d = \begin{bmatrix} \frac{\partial}{\partial x} & 0 \\ 0 & \frac{\partial}{\partial y} \\ \frac{\partial}{\partial y} & \frac{\partial}{\partial x} \end{bmatrix} \text{ for 2D,}$$

$$\mathbf{L}_d = \begin{bmatrix} \partial/\partial x & 0 & 0 \\ 0 & \partial/\partial y & 0 \\ 0 & 0 & \partial/\partial z \\ \partial/\partial y & \partial/\partial x & 0 \\ 0 & \partial/\partial z & \partial/\partial y \\ \partial/\partial z & 0 & \partial/\partial x \end{bmatrix} \text{ for 3D.} \quad (2)$$

In Eq. (1), $W_k(\mathbf{x} - \mathbf{x}_C)$ is a weight or smoothing function that satisfies the positivity and unity conditions:

$$W_k(\mathbf{x}-\mathbf{x}_C) \geq 0 \text{ and } \int_{\Omega_k^s} W_k(\mathbf{x}-\mathbf{x}_C) d\Omega = 1. \quad (3)$$

The following Heaviside-type function is the simplest, and most widely used as the smoothing function:

$$W_k(\mathbf{x}-\mathbf{x}_C) = \begin{cases} 1/V_k^s, & \mathbf{x} \in \Omega_k^s \\ 0, & \mathbf{x} \notin \Omega_k^s \end{cases}, \quad (4)$$

where $V_k^s = \int_{\Omega_k^s} d\Omega$ is the volume (for 3D) or the area (for 2D) or the length (for 1D) of the smoothing domain Ω_k^s . Substituting Eq. (4) into Eq. (1) and then using the divergence theorem, we obtain the smoothed strains:

$$\begin{aligned} \underbrace{\bar{\boldsymbol{\varepsilon}}_k}_{\text{constant in } \Omega_k^s} &= \frac{1}{V_k^s} \int_{\Omega_k^s} \mathbf{L}_d \mathbf{u}^h(\mathbf{x}) d\Omega \\ &= \frac{1}{V_k^s} \int_{\Gamma_k^s} \mathbf{L}_n(\mathbf{x}) \mathbf{u}^h(\mathbf{x}) d\Gamma, \end{aligned} \quad (5)$$

where \mathbf{u}^h is the assumed displacement vector, which is obtained using simply the PIM [5,6] in the S-FEM. When 3-noded triangular (Tr3) or 4-noded tetrahedral elements (Te4) are used, \mathbf{u}^h can also be computed using exactly the same way as in the FEM using the shape functions created based on the physical coordinate system [4]. $\mathbf{L}_n(\mathbf{x})$ is a matrix containing the components of the unit outward normal on the smoothing domain boundary Γ_k^s :

$$\mathbf{L}_n(\mathbf{x}) = n \text{ for 1D, } \mathbf{L}_n(\mathbf{x}) = \begin{bmatrix} n_x^s & 0 \\ 0 & n_y^s \\ n_y^s & n_x^s \end{bmatrix} \text{ for 2D,}$$

$$\mathbf{L}_n(\mathbf{x}) = \begin{bmatrix} n_x^s & 0 & 0 \\ 0 & n_y^s & 0 \\ 0 & 0 & n_z^s \\ n_y^s & n_x^s & 0 \\ 0 & n_z^s & n_y^s \\ n_z^s & 0 & n_x^s \end{bmatrix} \text{ for 3D,} \quad (6)$$

where n_x^s , n_y^s , and n_z^s are the unit outward normal components on Γ_k^s , respectively, on the x -, y -, and z -axis. It is shown in Eq. (5) that the strain is computed via integration rather than differentiation. This is the one “weakening” operation at the stage of strain approximation. We note here that when the smoothing domain shrinks to zero, we have

$$\bar{\boldsymbol{\varepsilon}}_k = \lim_{\Omega_k^s \rightarrow 0} \frac{1}{V_k^s} \int_{\Omega_k^s} \boldsymbol{\varepsilon}^h(\mathbf{x}) d\Omega = \boldsymbol{\varepsilon}^h(\mathbf{x}_C), \quad (7)$$

which means that the smoothed strain becomes the compatible strain, implying that the FEM is in fact a

special case of S-FEM at the limit when all the smoothing domains approach zero.

Apart from using the Heaviside-type function, one may use linear smoothing functions of equilateral triangle shape, as long as Eq. (3) is satisfied. In such a case, the smoothed strain is calculated via domain integration rather than a boundary integration.

2.2 Creation of different types of smoothed domains

S-FEM models use smoothed strains that are computed using Eq. (5) and the smoothing domains created on top of an element mesh. The art of the S-FEM is creative ways to form different types of smoothing domains, leading to different S-FEM models.

In a CS-FEM model, smoothing domains reside within the elements. In the CS-FEM using 4-noded quadrilateral (Q4) elements, for example, typical smoothing domains can be created by dividing the elements into smaller cells, as shown in Fig. 1, where one Q4 elements is divided into 1, 2, 3, 4, 8, or 16 smoothing cells (SCs). Each of the smoothing domains is bounded by four line boundary segments. In most applications, four SCs for each element are often used. Use of one SC can be more efficient and sometimes can produce upper bound solutions, but may have the so-called “hourglass” instability. It is also possible to used 4 SCs for some elements and 1 CS for other elements in the mesh, but this idea has not yet been implemented and studied in detail so far.

From Eq. (5), it is clear that the smoothing domain is used to evaluate the smoothed strains, the displacement values on the smoothing domain boundary is used in such evaluation, and the displacement values are interpolated using the nodal displacements. Because of this, the smoothed strains for the smoothing domain relate to all the nodes of the elements that have contribution to the smoothing domain. Such elements are called “supporting elements” and such nodes are called “supporting nodes” of the smoothing domain. For any smoothing cell in a Q4 element, the supporting element is 1, and the supporting nodes is 4.

Note that when Tr3-meshes are used, the CS-FEM will be exactly the same of as the FEM counterparts. This is because the compatible strains in Tr3 element is constant, and any cell-based smoothing operation can only produce the same constant smoothed strain. Similarly, when Te4-meshes are used, the 3D CS-FEM will be exactly the same as the 3D FEM counterparts.

When 3-noded triangular (Tr3) elements are used, one may create smoothing domains based on edges, leading to an ES-FEM-Tr3 models, as shown in Fig. 2 for 2D problems. In this case, each edge has a smoothing domain, and the total number of smoothing domains is exactly the number of edges in the mesh. A smoothing domain for an edge that is inside the problem domain, the edge-based

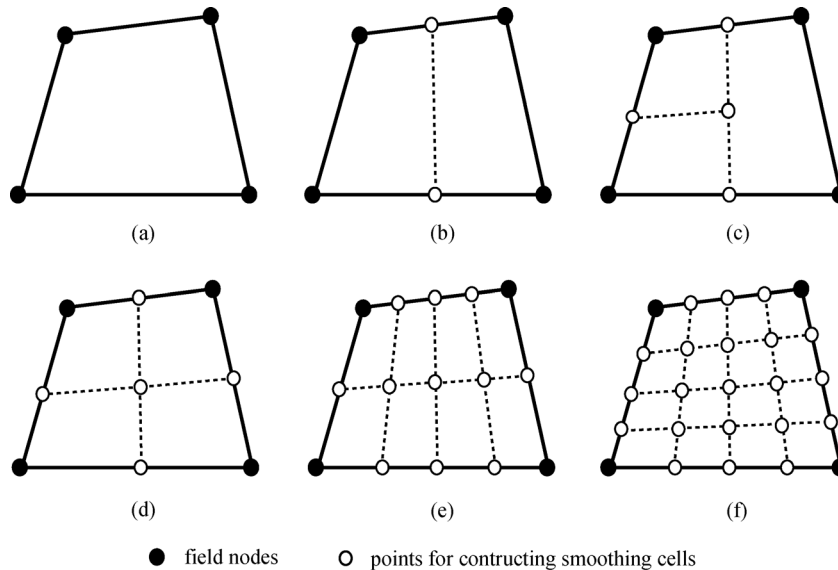


Fig. 1 Smoothing domains used in a CS-FEM model. A quadrilateral element may be divided into smoothing cells (SCs) by connecting the mid-segment-points of opposite segments of smoothing domains [36]. (a) $n_{SC} = 1$; (b) $n_{SC} = 2$; (c) $n_{SC} = 3$; (d) $n_{SC} = 4$; (e) $n_{SC} = 8$; (f) $n_{SC} = 16$ (from [98]). In applications, four SCs for each element are often used. Use of one SC can be more efficient and sometimes can produce upper bound solutions, but may have the so-called “hourglass” instability

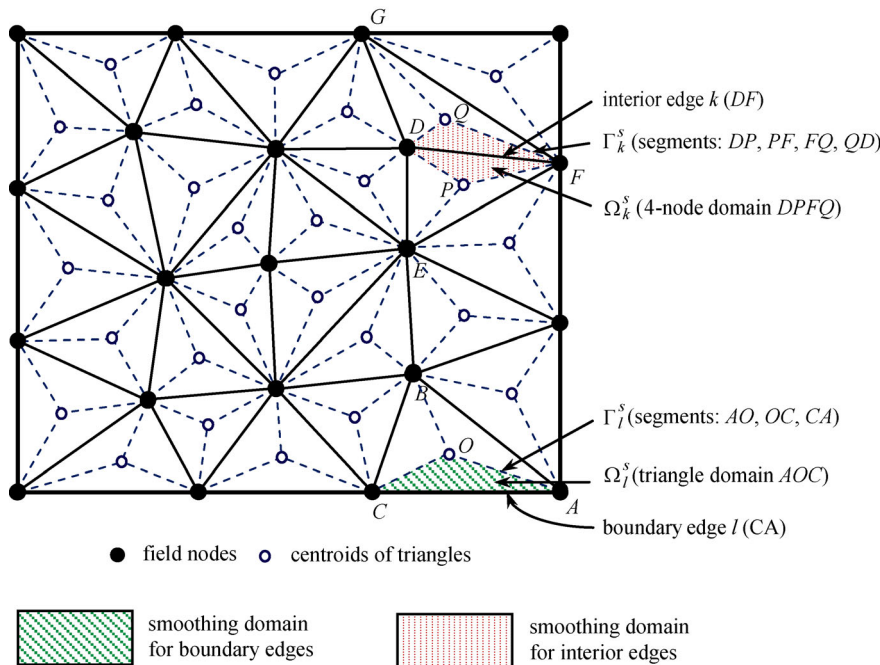


Fig. 2 Edge-based smoothing domains on a Tr3-mesh. Shaded areas are typical smoothing domains. The smoothing domain Ω_l^s is for edge l on the problem domain boundary, and is a triangle AOC for a boundary edge. Smoothing domain Ω_k^s is for interior edge k that is inside the problem domain, and it is a four-sided convex polygon $DPFQ$ (from Ref. [167])

smoothing domain is a four-sided polygon, the number of supporting elements is 2, and the smoothing domain boundary has 4 line segments. The number of supporting nodes of an interior edge-based smoothing domain is 4. For edge k , they are F, G, D , and E . For an edge on the problem domain boundary, and it is a triangle and the

smoothing domain boundary has only 3 line segments. The number of supporting element is 1, and the supporting nodes is 3 for a boundary edge-based smoothing domain. For edge l , these are A, O , and C .

An NS-FEM-Tr3 model uses node-based smoothing domains that are created based on nodes in a Tr3-mesh, as

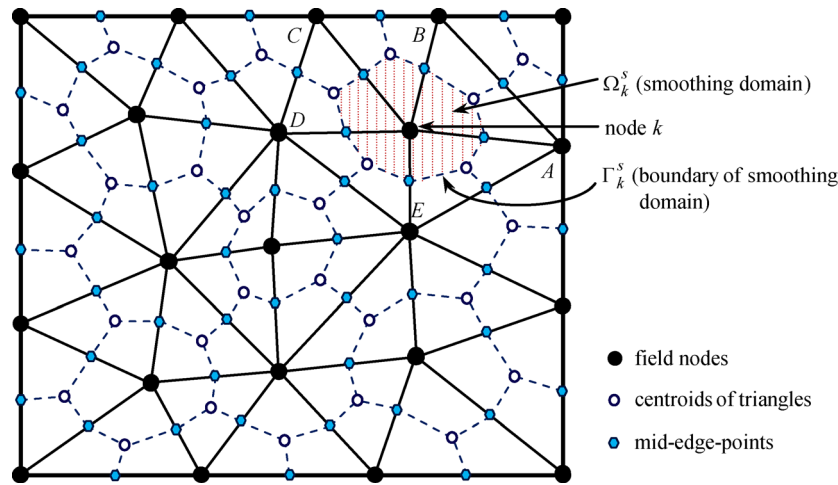


Fig. 3 Node-based smoothing domains for an NS-FEM model using Tr3-mesh. The smoothing domain Ω_k^s for node k is a polygon with $2n_k^e$ sides (where n_k^e is the number of elements surrounding node k) (from Ref. [167])

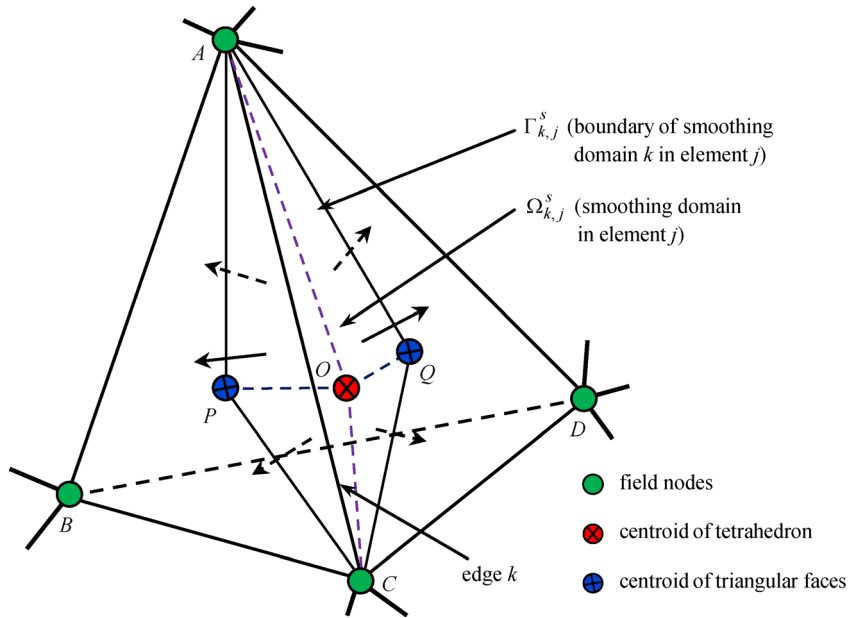


Fig. 4 Edge-based smoothing domain on a Te4-mesh for ES-FEM-Te4 model. Only the part of the smoothing domain $\Omega_{k,j}^s$ for edge k is shown. It is located inside element j , and is a double tetrahedron ACPOQ. If there are other elements connected to edge k , similar partial smoothing domains need to be constructed (from Ref. [167])

shown in Fig. 3. In this case, the number of the smoothing domain is the same as the number of all the nodes in the Tr3-mesh. A smoothing domain forms a polygon bounded by multiple line segments. Any segment connects the midpoint of an edge to a center of a Tr3 element connected to the node. For the shaded node-based smoothing domain shown in Fig. 3, it is supported by 5 elements and it is thus bounded by 10 line segments. The number of supporting nodes of the interior edge-based smoothing domain k is 6, and they are $A, B, C, D, E,$ and k . A node-based smoothing domain for a node on the problem boundary can be one-sided, and the number of supporting nodes is usually

smaller. In general a node-based smoothing domain may have contributions from any number of elements, as shown in Fig. 3. Mostly, one to seven elements.

For 3D problems, one may create edge-based S-FEM using 4-noded tetrahedral mesh, known as ES-FEM-Te4, as shown in Fig. 4. The supporting nodes of an edge-based smoothing domain are all the nodes of the element directly connected to the edge. We can also create node-based smoothing domains for NS-FEM-Te4 models, as shown in Fig. 5. In this case, the supporting nodes of a node-based smoothing domain are all the nodes of the element directly connected to the node. In addition, one may create

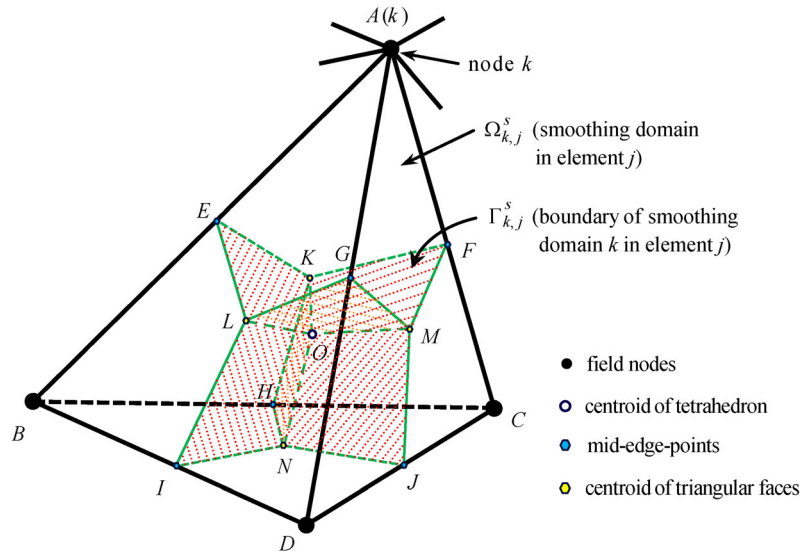


Fig. 5 Node-based smoothing domain on a part of Te4-mesh. Only part of the smoothing domain $\Omega_{k,j}^s$ is shown. It is for node k in the element j , and it is a polyhedron $AELGMFKO$. If there are other elements connected to node k , similar partial smoothing domains need to be constructed (from Ref. [167])

smoothing domains associated with the faces of the Te4 elements, known as the FS-FEM-Te4 model. Figure 6 shows a part of a face-based smoothing domain Ω_k^s created by connecting the three nodes of face (A,B,C) to the centers of these two neighboring elements (P,Q) . The supporting nodes of a face-based smoothing domain are all the nodes of the element directly connected to the face. For an interior face, the number of supporting nodes is 5, and for a face on the problem boundary, the number is 4, because only one Te4 element is involved in that smoothing domain.

Table 1 summaries several types of smoothing domains. More detailed procedure for constructing the smoothing domains can be found in Ref. [8].

Figures 7 and 8 show types of smoothing domains created on a 3D mechanical component (an engine

connection bar and socket, respectively) discretized with 4-noded tetrahedral elements, together with some solutions obtained using S-FEM models. Details on the formulation of an S-FEM model are given in the next Section.

2.3 S-FEM strain matrix (B-matrix)

We are now ready to form the strain-displacement matrix or B-matrix. For better clarity, we use 2D problem as an example. We write the assumed displacement $\mathbf{u}^h(\mathbf{x})$ in shape functions $\mathbf{N}_I(\mathbf{x})$ that satisfies the most essential condition of partitions of unity [199] and the nodal displacements \mathbf{d}_I for all the nodes of the elements contributing to the smoothing domain (SD):

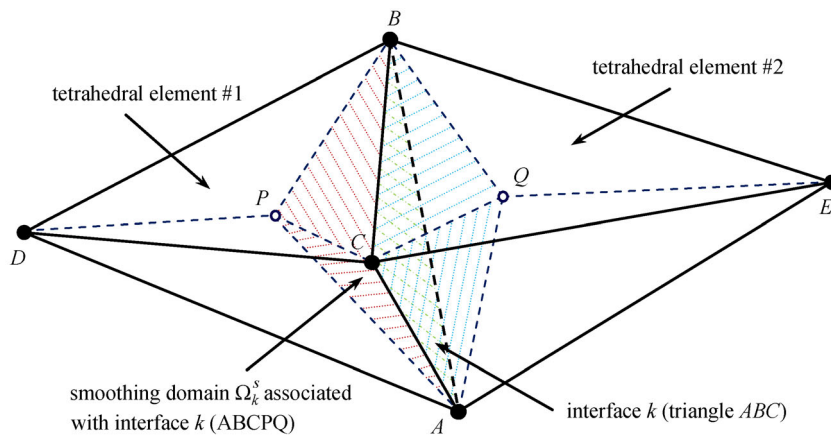


Fig. 6 Schematic illustration of face-based smoothing domains based on tetrahedral elements: a face-based smoothing domain Ω_k^s created from two adjacent tetrahedral elements based upon their interface k (from Ref. [167])

Table 1 Existing types of smoothing domains (SD's) used in S-FEM models

| Type* | method for creation and number of SD's (N_s) | S-FEM models | dimension of problem; properties |
|---------------------|--|----------------------|---|
| cell-based SD (CSD) | SD's or smoothing cells (SC's) are divided from and located within the elements ($N_s = \sum_{i=1}^{N_e} n_{sc}^i$, $n_{sc}^i = 1, 2, 3, 4, \dots$) | CS-FEM n CS-FEM | 1D, 2D, 3D softer; high accuracy; insensitive to mesh distortion |
| edge-based SD (ESD) | SD's are created based on edges by connecting portions of the surrounding elements sharing the associated edge ($N_s = N_{edge}$) | ES-FEM | 2D, 3D softer; very high accuracy; less insensitive to mesh distortion |
| node-based SD (NSD) | SD's are created based on nodes by connecting portions of the surrounding elements sharing the associated node ($N_s = N_{node}$) | NS-FEM | 1D, 2D, 3D soft; upper bound; very insensitive to mesh distortion; volumetric locking free |
| face-based SD (FSD) | SD's are created based on faces by connecting portions of the surrounding elements sharing the associated face ($N_s = N_{face}$) | FS-FEM | 3D softer; very high accuracy; less insensitive to mesh distortion |

*Note: There are S-FEM models that use combinations of different types of SDs, such as selective S-FEM, α FEM, and β FEM.

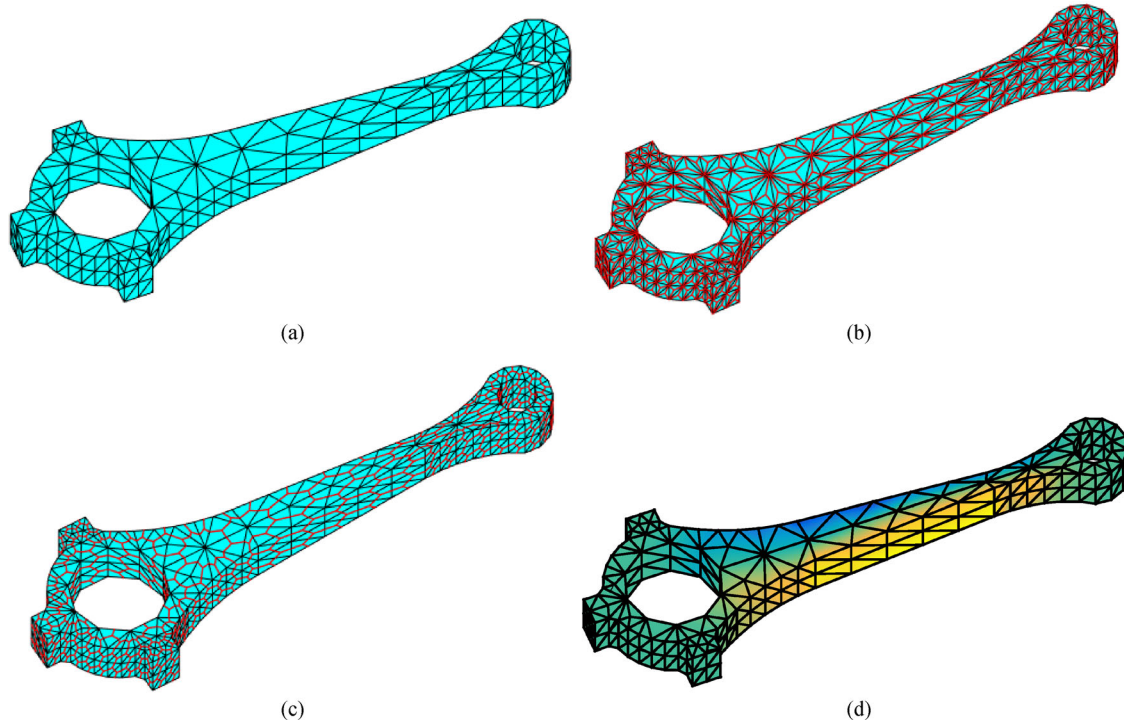


Fig. 7 Types of smoothing domains created on a 3D mechanical component (engine connection bar) discretized with 4-noded tetrahedral elements. (a) Face-based smoothing domains (on the surface the FS smoothing domains cannot be seen, and hence it appears like the element mesh); (b) edge-based smoothing domains; (c) node-based smoothing domains; (d) an example of a normal stress σ_{xx} solution using the ES-FEM-Te4 model [163]

$$\bar{\mathbf{e}}_k = \sum_{I \in S_k^n} \bar{\mathbf{B}}_{Ik} \mathbf{d}_{Ik}, \quad (8)$$

where S_k^n is the set of supporting nodes of Ω_k^s , and the smoothed B-matrix can be computed by

$$\bar{\mathbf{B}}_{Ik} = \frac{1}{V_k^s} \int_{\Gamma_k^s} \mathbf{n}^s(\mathbf{x}) \mathbf{N}_I(\mathbf{x}) d\Gamma = \begin{bmatrix} \bar{b}_{Ikx} & 0 & \bar{b}_{Iky} \\ 0 & \bar{b}_{Iky} & \bar{b}_{Ikx} \end{bmatrix}^T, \quad (9)$$

where V_k^s is the area of the k th smoothing domain.

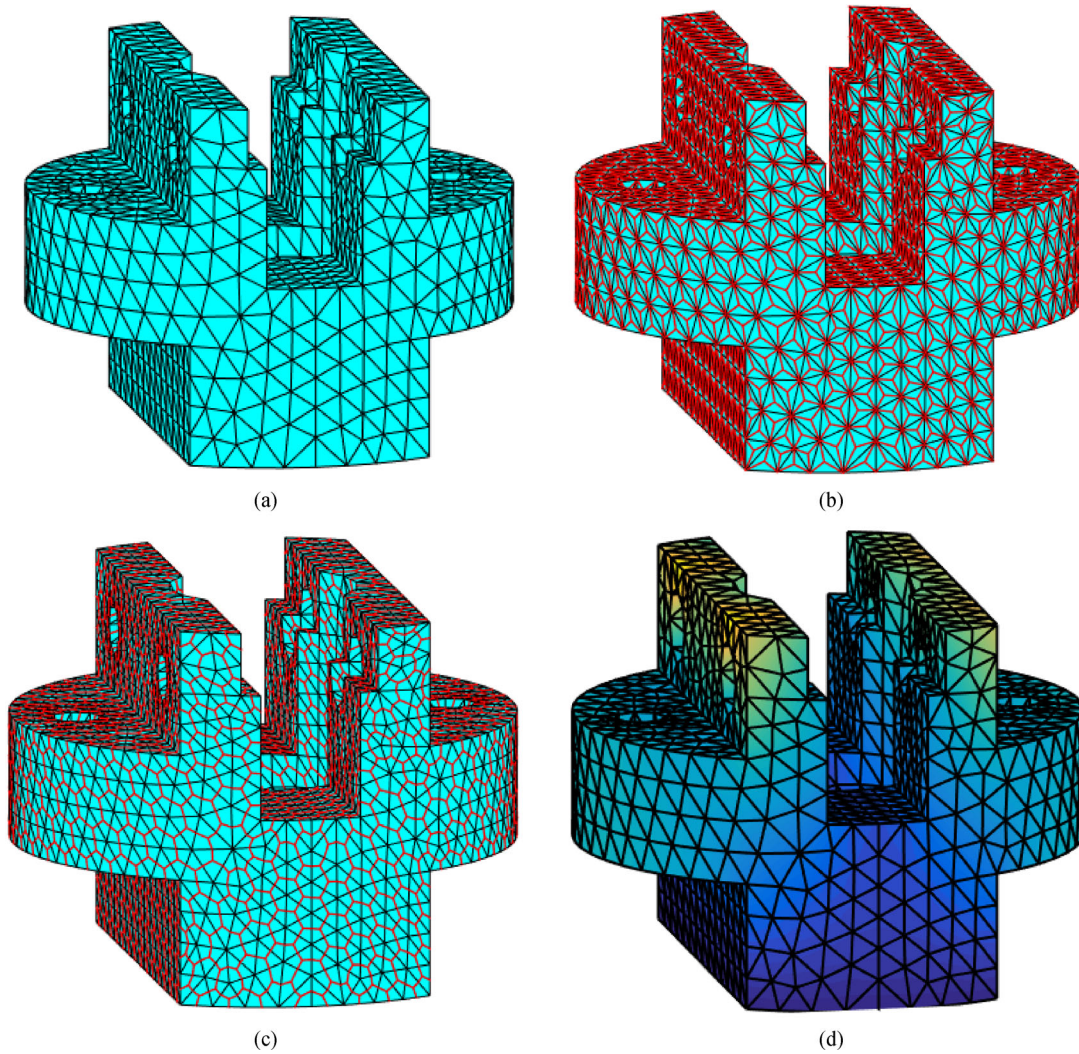


Fig. 8 Types of smoothing domains created on a 3D mechanical component (socket) discretized with 4-noded tetrahedral elements. (a) Face-based smoothing domains (on the surface the FS smoothing domains cannot be seen, and hence it appears like the element mesh); (b) edge-based smoothing domains; (c) node-based smoothing domains; (d) an example of a solution of displacement in the z -direction using the FS-FEM-Te4 model [163]

$$\begin{aligned} \bar{b}_{lkh} &= \frac{1}{V_k^s} \int_{\Gamma_k^s} N_l(\mathbf{x}) n_h^s(\mathbf{x}) d\Gamma \\ &= \frac{1}{V_k^s} \sum_{p=1}^{n_r^s} n_{h,p}^s N_l(\mathbf{x}_p^G) l_p^s, \quad h = x, y, \end{aligned} \quad (10)$$

in which n_r^s is the total number of the boundary segments $\Gamma_{k,p}^s \in \Gamma_k^s$, \mathbf{x}_p^G is the Gauss point on $\Gamma_{k,p}^s$. The length and outward unit normal of $\Gamma_{k,p}^s$ are denoted as l_p^s and $n_{h,p}^s$, respectively. Here we use 1-point Gauss quadrature to numerically perform the integration along each segment. It is clearly seen in Eq. (10) that in computing B-matrix, derivatives of shape functions N_l are not required, and we need only the shape functions values and only for the points on the SD boundary segments. Once the SDs are

created, one knows exactly the supporting elements and nodes for each SD, and hence the shape function values for all the supporting nodes at any point on the SD boundary segments can be easily computed using the PIM [6,8]. The compatibility is not a concern at all for an S-FEM model. This is because the PIM is performed for points on the SD boundary, it satisfies the continuity requirement for any function being in a G_h^1 space, and hence the stability is ensured [5,6].

For the case of using 4 SDs in a Q4 element (shown in Fig. 9), the values of the 4 nodal shape functions at the 12 Gauss points on these boundary segments of the 4 SDs can be computed by simple PIM (in fact a simple inspection), as listed in the Table 3 [8]. The key point here is that we do not need to construct these shape functions of each of these 4 nodes (this would be, in fact, a nontrivial task, because it

Table 2 Minimum number of smoothing domains N_s^{\min} for solid mechanics problems with n_t (unconstrained) total nodes [5,8]

| dimension of the problem | minimum number of smoothing domains |
|--------------------------|-------------------------------------|
| 1D | $N_s^{\min} = n_t$ |
| 2D | $N_s^{\min} = 2n_t/3$ |
| 3D | $N_s^{\min} = 3n_t/6 = n_t/2$ |

needs on in the physical coordinate system, and hence mapping is required as in the FEM). Note also that mapping is not required in S-FEM. Therefore, it is more computationally efficient and simpler in this regards. Such a PIM can also be used for any arbitrary polygonal elements, as the 6-sided polygonal element shown in Fig. 9 (a), and the results for all these Gauss points are listed in Table 4.

Note that the summation in Eq. (8) is in fact an “assembly” or a “node-matched” summation. As an example, let us consider an ES-FEM model for 2D problems. In this case, the (shaded) edge-based SD $DPFQ$ shown in Fig. 2 is supported by 4 nodes D, E, F, G from two Tr3 elements DEF and DFG . The smoothed B-matrix for the whole SD Ω_k^s can then be written as Ref. [8]

$$\bar{\mathbf{B}}_k = [\bar{\mathbf{B}}_{Dk} \bar{\mathbf{B}}_{Ek} \bar{\mathbf{B}}_{Fk} \bar{\mathbf{B}}_{Gk}]. \tag{11}$$

All these sub-matrices in the right-hand-side of the forgoing equation can be computed easily using Eqs. (9) and (10). For the ES-FEM-T3 model, only one Gauss point is required along any boundary segment, because the shape function changes linearly and the unit normal vector is a constant along the segments.

For Tr3 elements, the area of a SD can be calculated using the areas of the elements supporting the SD:

$$V_k^s = \int_{\Omega_k^s} d\Omega = \frac{1}{3} \sum_{j=1}^{n_k^e} V_j^e, \tag{12}$$

where n_k^e is the number of elements connected to edge k and V_j^e is the area of an element.

The above is the standard way to compute the smoothed B-matrix. Alternatively, one may use the area-weighted summation method, if Tr3 elements and linear PIM is used. In this method, $\bar{\mathbf{B}}_{Ik}$ is computed using directly all the compatible FE \mathbf{B}_I^{e-j} for the j th element that is connected to edge k . \mathbf{B}_I^{e-j} for node I can be evaluated using the shape function of node I in the j th element:

Table 3 Values of 4 nodal shape functions at different points within a Q4 element [8] (shown in Fig. 9(a))

| point | N_1 | N_2 | N_3 | N_4 | description |
|-------|-------|-------|-------|-------|--|
| 1 | 1.0 | 0 | 0 | 0 | field node |
| 2 | 0 | 1.0 | 0 | 0 | field node |
| 3 | 0 | 0 | 1.0 | 0 | field node |
| 4 | 0 | 0 | 0 | 1.0 | field node |
| 5 | 1/2 | 1/2 | 0 | 0 | side midpoint |
| 6 | 0 | 1/2 | 1/2 | 0 | side midpoint |
| 7 | 0 | 0 | 1/2 | 1/2 | side midpoint |
| 8 | 1/2 | 0 | 0 | 1/2 | side midpoint |
| 9 | 1/4 | 1/4 | 1/4 | 1/4 | intersection of two bi-medians |
| g1 | 3/4 | 1/4 | 0 | 0 | Gauss point (mid-segment point of $\Gamma_{k,p}^x$) |
| g2 | 3/8 | 3/8 | 1/8 | 1/8 | Gauss point (mid-segment point of $\Gamma_{k,p}^x$) |
| g3 | 3/8 | 1/8 | 1/8 | 3/8 | Gauss point (mid-segment point of $\Gamma_{k,p}^x$) |
| g4 | 3/4 | 0 | 0 | 1/4 | Gauss point (mid-segment point of $\Gamma_{k,p}^x$) |
| g5 | 1/4 | 3/4 | 0 | 0 | Gauss point (mid-segment point of $\Gamma_{k,p}^x$) |
| g6 | 0 | 3/4 | 1/4 | 0 | Gauss point (mid-segment point of $\Gamma_{k,p}^x$) |
| g7 | 1/8 | 3/8 | 3/8 | 1/8 | Gauss point (mid-segment point of $\Gamma_{k,p}^x$) |
| g8 | 0 | 1/4 | 3/4 | 0 | Gauss point (mid-segment point of $\Gamma_{k,p}^x$) |
| g9 | 0 | 0 | 3/4 | 1/4 | Gauss point (mid-segment point of $\Gamma_{k,p}^x$) |
| g10 | 1/8 | 1/8 | 3/8 | 3/8 | Gauss point (mid-segment point of $\Gamma_{k,p}^x$) |
| g11 | 0 | 0 | 1/4 | 3/4 | Gauss point (mid-segment point of $\Gamma_{k,p}^x$) |
| g12 | 1/4 | 0 | 0 | 3/4 | Gauss point (mid-segment point of $\Gamma_{k,p}^x$) |

Table 4 Values of six nodal shape functions at different points within a 6-sided polygonal element [8] (shown in Fig. 9(b))

| point | N_1 | N_2 | N_3 | N_4 | N_5 | N_6 | description |
|----------|-------|-------|-------|-------|-------|-------|--|
| 1' | 1.0 | 0 | 0 | 0 | 0 | 0 | field node |
| 2' | 0 | 1.0 | 0 | 0 | 0 | 0 | field node |
| 3' | 0 | 0 | 1.0 | 0 | 0 | 0 | field node |
| 4' | 0 | 0 | 0 | 1.0 | 0 | 0 | field node |
| 5' | 0 | 0 | 0 | 0 | 1.0 | 0 | field node |
| 6' | 0 | 0 | 0 | 0 | 0 | 1.0 | field node |
| O | 1/6 | 1/6 | 1/6 | 1/6 | 1/6 | 1/6 | centroid point |
| g1' | 7/12 | 1/12 | 1/12 | 1/12 | 1/12 | 1/12 | Gauss point (mid-segment point of $\Gamma_{k,p}^s$) |
| g2' | 1/2 | 1/2 | 0 | 0 | 0 | 0 | Gauss point (mid-segment point of $\Gamma_{k,p}^s$) |
| g3' | 1/12 | 7/12 | 1/12 | 1/12 | 1/12 | 1/12 | Gauss point (mid-segment point of $\Gamma_{k,p}^s$) |
| g4' | 0 | 1/2 | 1/2 | 0 | 0 | 0 | Gauss point (mid-segment point of $\Gamma_{k,p}^s$) |
| g5' | 1/12 | 1/12 | 7/12 | 1/12 | 1/12 | 1/12 | Gauss point (mid-segment point of $\Gamma_{k,p}^s$) |
| g6' | 0 | 0 | 1/2 | 1/2 | 0 | 0 | Gauss point (mid-segment point of $\Gamma_{k,p}^s$) |
| g7' | 1/12 | 1/12 | 1/12 | 7/12 | 1/12 | 1/12 | Gauss point (mid-segment point of $\Gamma_{k,p}^s$) |
| g8' | 0 | 0 | 0 | 1/2 | 1/2 | 0 | Gauss point (mid-segment point of $\Gamma_{k,p}^s$) |
| g9' | 1/12 | 1/12 | 1/12 | 1/12 | 7/12 | 1/12 | Gauss point (mid-segment point of $\Gamma_{k,p}^s$) |
| g10' | 0 | 0 | 0 | 0 | 1/2 | 1/2 | Gauss point (mid-segment point of $\Gamma_{k,p}^s$) |
| g11' | 1/12 | 1/12 | 1/12 | 1/12 | 1/12 | 7/12 | Gauss point (mid-segment point of $\Gamma_{k,p}^s$) |
| g12' | 1/2 | 0 | 0 | 0 | 0 | 1/2 | Gauss point (mid-segment point of $\Gamma_{k,p}^s$) |

$$\mathbf{B}_I^{e,j} = \mathbf{L}_d \mathbf{N}_I(\mathbf{x}). \tag{13}$$

The sub-smoothed B-matrix for node I is then computed using

$$\bar{\mathbf{B}}_{Ik} = \frac{1}{V_k^s} \sum_{j=1}^{n_k^e} \left[\frac{1}{3} V_j^e \mathbf{B}_I^{e,j} \right]. \tag{14}$$

For the example in Fig. 2, elements DEF and DFG

$$\bar{\mathbf{B}}_k = \left[\underbrace{\frac{1}{3} \mathbf{B}_D^{e,DEF} + \frac{1}{3} \mathbf{B}_D^{e,DEG}}_{\bar{\mathbf{B}}_{Dk}} \quad \underbrace{\frac{1}{3} \mathbf{B}_E^{e,DEF}}_{\bar{\mathbf{B}}_{Ek}} \quad \underbrace{\frac{1}{3} \mathbf{B}_F^{e,DEF} + \frac{1}{3} \mathbf{B}_F^{e,DEG}}_{\bar{\mathbf{B}}_{Fk}} \quad \underbrace{\frac{1}{3} \mathbf{B}_G^{e,DEG}}_{\bar{\mathbf{B}}_{Gk}} \right]. \tag{15}$$

We noted that Eqs. (11) and (15) are identical, if Tr3 elements (linear PIM) are used. Equation (11) is standard and applicable to other types of elements and higher order PIMs (with of course more Gauss points for the integrations).

2.4 S-FEM stiffness matrix

The computation and formation of the smoothed stiffness matrix $\bar{\mathbf{K}}$ is quite similar to those procedures in the

support the red shaded SD Ω_k^s . However, element DFG is not related to node E . When $\bar{\mathbf{B}}_{Ek}$ is computed, it has only 1/3 contribution of $\mathbf{B}_E^{e,DEF}$ from element DEF . Likewise, when $\bar{\mathbf{B}}_{Gk}$ is computed, 1/3 of $\mathbf{B}_G^{e,DEG}$ is contributed from DFG . However, when $\bar{\mathbf{B}}_{Dk}$ or $\bar{\mathbf{B}}_{Fk}$ is computed, we have contributions from both elements, as they all share nodes D and F . The smoothed B-matrix for the whole SD Ω_k^s can be written in the following form.

standard FEM. It can be assembled from the contributions of the sub-stiffness-matrices from all the smoothing domains,

$$\begin{aligned} \bar{\mathbf{K}}_{IJ} &= \int_{\Omega} \bar{\mathbf{B}}_I^T \mathbf{c} \bar{\mathbf{B}}_J d\Omega = \sum_{k=1}^{N_s} \left[\int_{\Omega_k^s} \bar{\mathbf{B}}_{Ik}^T \mathbf{c} \bar{\mathbf{B}}_{Jk} d\Omega \right] \\ &= \sum_{k=1}^{N_s} \underbrace{\bar{\mathbf{B}}_{Ik}^T \mathbf{c} \bar{\mathbf{B}}_{Jk}}_{\mathbf{K}_{Ijk}} V_k^s, \end{aligned} \tag{16}$$

The summation is a node-matched summation at the stiffness matrix level. The derivation of the above equation is similar as that in the FEM. The main difference is that FEM is *element* based, while the S-FEM is *smoothing-domain* based. The existing assembly algorithms in the FEM can be used for S-FEM by simply treating the smoothing domains as “elements”. When I and J are “far” apart, $\bar{\mathbf{K}}_{IJ}$ vanishes. Thus, the global stiffness matrix $\bar{\mathbf{K}}$ is a sparse (assuming it is formed). It is banded when the nodes are properly numbered.

2.5 S-FEM discretized system equations

Consider now dynamic problems for solids and structures, the discretized system of equations in an S-FEM can be expressed as the following set of 2nd order differential equations with respect to time.

$$\bar{\mathbf{K}}\mathbf{d} + \tilde{\mathbf{C}}\dot{\mathbf{d}} + \tilde{\mathbf{M}}\ddot{\mathbf{d}} = \tilde{\mathbf{f}}, \quad (17)$$

where $\tilde{\mathbf{M}}$ is the mass matrix obtained using

$$\tilde{\mathbf{M}} = \int_{\Omega} \mathbf{N}^T \rho \mathbf{N} d\Omega, \quad (18)$$

in which ρ is the mass density, and \mathbf{N} is the matrix of nodal shape functions of all nodes [4,8]. Matrix $\tilde{\mathbf{C}}$ is the damping matrix computed using

$$\tilde{\mathbf{C}} = \int_{\Omega} \mathbf{N}^T c_d \mathbf{N} d\Omega, \quad (19)$$

where c_d is the damping coefficient of the material. Vector $\tilde{\mathbf{f}}$ is the external force vector acting at all the nodes in the problem domain. It has entries of

$$\tilde{\mathbf{f}}_I = \int_{\Omega} \mathbf{N}_I^T(\mathbf{x}) \mathbf{b} d\Omega + \int_{\Gamma_f} \mathbf{N}_I^T(\mathbf{x}) \mathbf{t} d\Gamma, \quad (20)$$

where \mathbf{b} is the distributed body force vector, and the \mathbf{t} is the traction vector applied on the force boundary of the problem domain.

In the S-FEM, the smoothing operation is only applied to the derivatives of the displacement (or shape) functions. We do not perform any additional treatments to the displacement function itself. Therefore, the mass matrix, damping matrix, and the force vectors are computed in exactly the same way as in the standard FEM. The damping matrix may also be modeled as in the standard FEM. For example using the so-called Rayleigh damping. In such a case the damping matrix $\tilde{\mathbf{C}}$ is assumed to be a linear combination of $\tilde{\mathbf{M}}$ and $\bar{\mathbf{K}}$,

$$\tilde{\mathbf{C}} = \alpha \tilde{\mathbf{M}} + \beta \bar{\mathbf{K}}, \quad (21)$$

where α and β are the Rayleigh damping coefficients determined by experiments.

The stiffness matrix $\bar{\mathbf{K}}$ is a symmetric positive definite (SPD), after sufficient displacement boundary conditions are imposed [4,8], as long as the number of the smoothing domains satisfy the following table of stability conditions.

The bandwidth of $\bar{\mathbf{K}}$ depends on the types of S-FEM model. For CS-FEM-Q4, it is the same as the FEM. For ES-FEM-Tr3, the bandwidth is about 30% larger than the FEM counterpart. For NS-FEM-Tr3, the bandwidth is doubled. Therefore, if direct solver is used for Eq. (17), NS-FEM is expected slower than ES-FEM that is also slower than the FEM counterpart using the same mesh. The S-FEM can, however, stand out by producing more accurate solutions and/or offering unique solution properties.

Note that when explicit solver is used for dynamic problems, we do not need to form matrix $\bar{\mathbf{K}}$ during the computation. In such cases, the computation time is largely determined by the number of smoothing domains (elements in the case of FEM). In this case, NS-FEM can be faster than ES-FEM that is also faster than the FEM counterpart using the same mesh. This is because for a mesh the number of nodes is usually smaller than the number of elements and that even smaller than the number of edges. The S-FEM can also stand out further by producing more accurate solutions or offer unique solution properties.

3 Solution properties of S-FEM models

3.1 Example 1: 2D cantilever beam

Next we study a benchmarking mechanics problem known as 2D cantilever beam, which has an analytical solution given in [8,191]. The beam is a simple rectangular shape with a length $L = 48$ m and height $D = 12$ m is subjected to a parabolic traction at the free end as in Fig. 10. When we assume the thickness is very small comparing with its height, and thus it is considered as a 2D plane-stress problem. Because we have exact solution, we can use it to examine our numerical models in detail.

Convergence of numerical solution in the strain energy are obtained using various numerical methods for this 2D cantilever problem, and the results are plotted in Fig. 11. A set of uniformly distributed 3-noded triangular elements are used to discretize the problem domain, and the density of the mesh is controlled by the DoFs. It is found that the FEM solution produces a lower bound, the NS-FEM gives an upper bound, and the ES-FEM gives ultra-accurate solution. All these numerical models use exactly the same element mesh, but different types of smoothing domains (note that the FEM is in fact the same as CS-FEM-Tr3). The findings from this example are in-line with the predictions by our S-FEM theory. This demonstrates an important point that we can now design numerical models

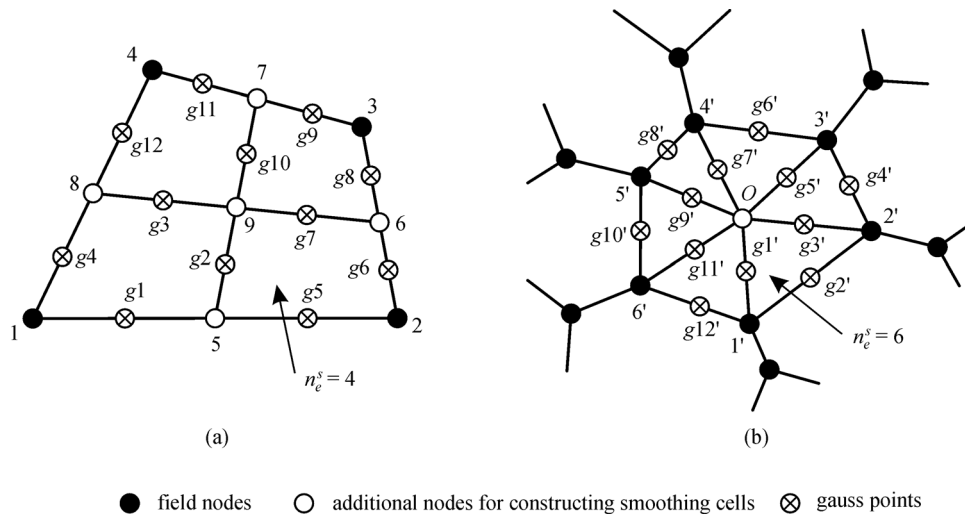


Fig. 9 Positions of Gauss points at mid-segment-points on segments of smoothing domains. (a) Four quadrilateral smoothing domains in a Q4 element; (b) six triangular smoothing domains in a 6-sided polygonal element (from Ref. [8])

with different properties by simply using different types of smoothing domains.

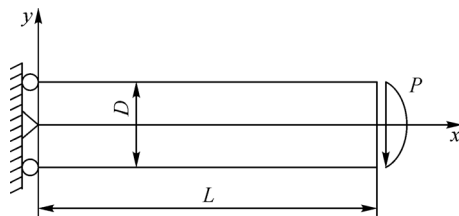


Fig. 10 A 2D cantilever beam loaded by a downward parabolically distributed shear stress at the right end

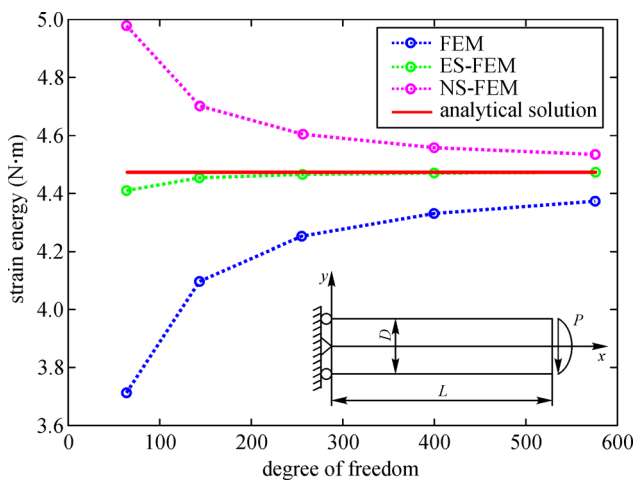


Fig. 11 Convergence of numerical solution in the strain energy for the 2D cantilever problem (from Ref. [163])

3.2 Example 2: 3D cantilever cubic solid

We next consider a 3D mechanics problem of cantilever

cubic solid. Its three dimensions are $L = W = H = 1\text{ m}$, and it is subjected to a uniform pressure loading on the upper face shown in Fig. 12. The cubic solid is fixed on its left face. Young’s modulus of the solid material is $E = 1.0 \times 10^3 \text{ N/m}^2$ and Poisson’s ratio is $\nu = 0.3$. This problem seems simple, but there is no exact solution to it. To conduct a detailed analysis for our numerical methods, we need to use a reference solution. Almeida Pereira has provided such a solution using a solution obtained with a very fine mesh of hexahedral super-elements, together with a procedure of Richardson’s extrapolation [191]. Such a reference solution is a good approximation of the exact solution and are used by many for examining numerical models. The solution in strain energy is 0.95093.

Figure 13 plots the convergence curves of numerical solutions obtained using different numerical models in

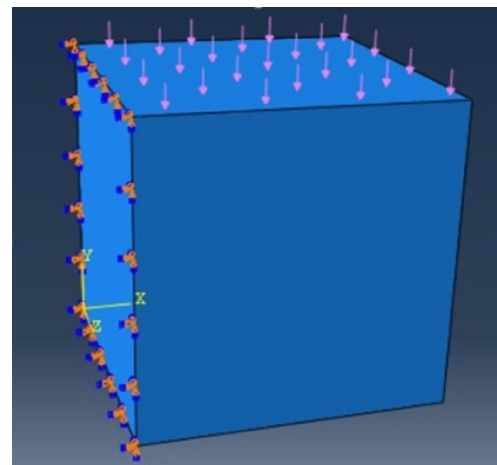


Fig. 12 A 3D cantilever cubic solid fixed on its left face, and it is subjected to a uniformly distributed pressure loading on the top surface

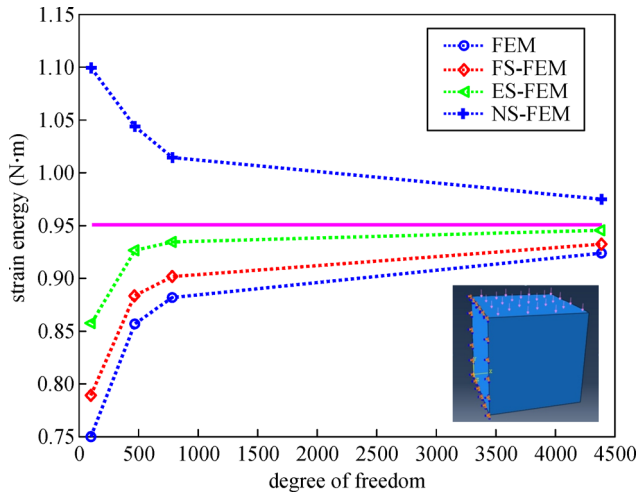


Fig. 13 Convergence of numerical solution in strain energy for the 3D cantilever cubic solid (from Ref. [163])

strain energy for the 3D cantilever cubic solid. A set of uniformly distributed 4-noded tetrahedral elements are used to discretize the problem domain, and the density of the mesh is controlled by the DoFs. It is found again that the FEM solution is a lower bound, the NS-FEM gives an upper bound, and the ES-FEM gives ultra-accurate solution. The solution from the FS-FEM is also much more accurate than the FEM counterpart. The all use exactly the same element mesh, but different types of smoothing domain. The findings are again in-line with the predictions by the S-FEM theory. This demonstrates again that we can now design numerical models with different properties by simply using different types of smoothing domains.

Figure 14 shown an important and useful idea based on the properties of S-FEM models. In the S-FEM framework, we have now two knobs: one tuns the stiffening effects by properly assuming the displacement field for the model, and another tuns the softening effects by strain smoothing operations (via using different types of smoothing domains). To obtain an lower bound solution, we tun up

the left knob, and to obtained a upper bound solution, we tun the right knob. In theory, one can produce an S-FEM model by design that can produce exact solution at least in a norm for a mechanics problem for solids and structures.

4 Moving forward

The development of S-FEM has already opened a new window of opportunity to develop the next generation of computational methods. Moving forward, it is the author’s opinion that the S-FEM will advances fast in the following areas:

1) Development of commercial software packages using S-FEM technology. Because S-FEM works well with T-mesh, we need now only use T-mesh that can be automatically generated for complex geometry. This is also extremely important for our dream for fully-automation in computation, modeling, and simulation. The manual operations from the analyst of a project will be drastically reduced. S-FEM software and the pre-processes can also be much simpler compared to the FEM counterpart, because of the use of simplest T-mesh. Some of the basic S-FEM codes for various models are available for free download (a simple registration for records is needed) at GRLab’s website, which offers a good initial starting point.

2) The automation capability of S-FEM offers conveniences in creating real-time AI models for mechanics problems, based on neural networks [207,208]. The AI methods are basically data-based, and the current biggest bottleneck problem with AI is the difficulty to obtain a large number of training samples. The S-FEM is physics-based, and it can be used for generating training samples for neural networks, by creating automatically S-FEM models using T-meshes. Because manual operations are drastically reduced for model creation, one can create as many training samples as needed. This is particularly important for inverse problems [209].

3) A lot more intensive applications of S-FEM is expected in practical applications in sciences and engi-

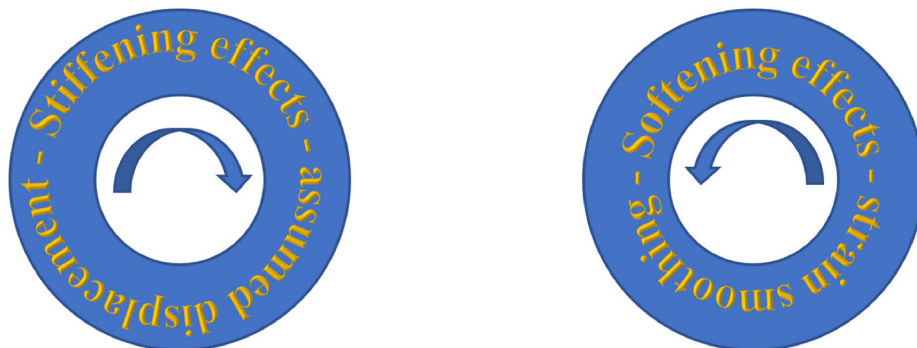


Fig. 14 In the S-FEM framework, we have now two knobs: one on the left tuns the stiffening effects by properly assuming the displacement field for the model, and another on the right tuns the softening effects by strain smoothing operations

neering fields, especially problems require adaptive analyses. Even more innovative ways to construct new types of smoothing domains. So far the smoothing domains in the existing S-FEM models are created in tight relations with the element mesh. This is not necessary. In theory, the smoothing domains can be independent of element mesh. A recent work by Liu's group has made some initial attempt in this direction [210].

4) Higher order S-FEM models. The S-FEM models developed so far are mainly linear models (linear PIM shape functions, and SD-based piecewise linear strain field). Such linear S-FEM models shall suffice for most of the applications (based on our experiences in using FEM, linear and bilinear models are most widely used, even though higher FEM elements are available in most software packages). However, higher order models will be an important addition. Liu has recently developed a *pick-out theory* and a systematic approach to construct higher order smoothed strain field [211]. The development of higher order S-FEM models is already on the way. The use of robust radial basis functions can also be a new direction of development for more robust and higher order formulations [194,200].

5) Most importantly we may need to develop ideas to make full use of the S-FEM frame work that enables us to develop models in convenient manner based the demand of the analyst on the required solution property. This requires a change on the perception of a numerical model.

5 Concluding remarks

This article first provides a brief review on the widely used FEM, and then a concise and easy-to-following presentation of key minimum necessary formulae used in the S-FEM. Following this concise introduction, reader shall be able to understand the essence of S-FEM and code S-FEM models based on the basic codes provided at GRLab's website. We provided also new directions on further development of S-FEM technology.

A number of important properties and unique features of S-FEM models are discussed in detail, which helps readers to understand better and appreciate the method. Most importantly, a concept of numerical model on-demand based on the S-FEM framework is proposed that may drastically change the landscape of modeling and simulation. One can in fact purposely design an S-FEM model to obtain solutions with special properties. This changes the perception of a numerical model. We used to treat a numerical model as merely tool for analysis to optimize our product design. With the S-FEM framework, we can now have a means to optimize the tool itself for desired solutions, which can next be utilized for much more reliable analyses and then to optimize our product design with high confidence. For example, for an automatically

generated T-mesh, one can create automatically different types of smoothing domains [163,190]. By invoking NS-FEM one gets upper bound solution, FEM for lower bound solution, and ES-FEM for solutions with high accuracy. This new concept of numerical model On-Demand is valuable for full automation in computations and adaptive analyses, and hence has profound impact on the future AI-assisted modeling and simulation.

References

1. Hughes T J R. The Finite Element Method: Linear Static and Dynamic Finite Element Analysis. Englewood Cliffs: Prentice-Hall, 1987
2. Belytschko T, Liu W K, Moran B, Elkhodary K I. Nonlinear Finite Elements for Continua and Structures, 2nd ed. West Sussex: Wiley, 2014
3. Bathe K J. Finite Element Procedures. Englewood Cliffs: Prentice-Hall, 1996
4. Liu G R, Quek S S. The Finite Element Method: A Practical Course, 2nd ed. Oxford: Butterworth-Heinemann, 2013
5. Liu G R. Meshfree Methods: Moving Beyond the Finite Element Method, 2nd ed. Boca Raton: CRC Press, 2009
6. Liu G R, Zhang G Y. The Smoothed Point Interpolation Methods – G Space Theory and Weakened Weak Forms. New Jersey: World Scientific Publishing, 2013
7. Liu G R. An overview on meshfree methods: for computational solid mechanics. International Journal of Computational Methods, 2016, 13(05): 1630001
8. Liu G R, Nguyen-Thoi T. Smoothed Finite Element Methods. Boca Raton: CRC Press, 2010
9. Liu G R, Zhang G Y, Dai K Y, Wang Y Y, Zhong Z H, Li G Y, Han X. A linearly conforming point interpolation method (LC-PIM) for 2D solid mechanics problems. International Journal of Computational Methods, 2005, 2(4): 645–665
10. Zhang G Y, Liu G R, Wang Y Y, Huang H T, Zhong Z H, Li G Y, Han X. A linearly conforming point interpolation method (LC-PIM) for three-dimensional elasticity problems. International Journal for Numerical Methods in Engineering, 2007, 72(13): 1524–1543
11. Liu G R, Zhang G Y. Upper bound solution to elasticity problems: a unique property of the linearly conforming point interpolation method (LC-PIM). International Journal for Numerical Methods in Engineering, 2008, 74(7): 1128–1161
12. Liu G R, Dai K Y, Nguyen-Thoi T. A smoothed finite element method for mechanics problems. Computational Mechanics, 2007, 39(6): 859–877
13. Liu G R, Nguyen T T, Dai K Y, Lam K Y. Theoretical aspects of the smoothed finite element method (SFEM). International Journal for Numerical Methods in Engineering, 2007, 71(8): 902–930
14. Dai K Y, Liu G R. Free and forced vibration analysis using the smoothed finite element method (SFEM). Journal of Sound and Vibration, 2007, 301(3–5): 803–820
15. Dai K Y, Liu G R, Nguyen-Thoi T. An n -sided polygonal

- smoothed finite element method (nSFEM) for solid mechanics. *Finite Elements in Analysis and Design*, 2007, 43(11–12): 847–860
16. Nguyen-Thoi T, Liu G R, Dai K Y, Lam K Y. Selective smoothed finite element method. *Tsinghua Science and Technology*, 2007, 12 (5): 497–508
 17. Liu G R. A generalized gradient smoothing technique and the smoothed bilinear form for Galerkin formulation of a wide class of computational methods. *International Journal of Computational Methods*, 2008, 5(2): 199–236
 18. Liu G R, Nguyen-Thoi T, Lam K Y. A novel alpha finite element method (α FEM) for exact solution to mechanics problems using triangular and tetrahedral elements. *Computer Methods in Applied Mechanics and Engineering*, 2008, 197(45–48): 3883–3897
 19. Cui X Y, Liu G R, Li G Y, Zhao X, Nguyen T T, Sun G Y. A smoothed finite element method (SFEM) for linear and geometrically nonlinear analysis of plates and shells. *CMES: Comput Model Eng Sci*, 2008, 28: 109–125
 20. Liu G R, Nguyen-Thoi T, Nguyen-Xuan H, Lam K Y. A node-based smoothed finite element method (NS-FEM) for upper bound solutions to solid mechanics problems. *Computers & Structures*, 2009, 87(1–2): 14–26
 21. Liu G R, Nguyen-Thoi T, Lam K Y. An edge-based smoothed finite element method (ES-FEM) for static, free and forced vibration analyses of solids. *Journal of Sound and Vibration*, 2009, 320(4–5): 1100–1130
 22. He Z C, Liu G R, Zhong Z H, Wu S C, Zhang G Y, Cheng A G. An edge-based smoothed finite element method (ES-FEM) for analyzing three-dimensional acoustic problems. *Computer Methods in Applied Mechanics and Engineering*, 2009, 199(1–4): 20–33
 23. Cui X Y, Liu G R, Li G Y, Zhang G Y, Sun G Y. Analysis of elastic-plastic problems using edge-based smoothed finite element method. *International Journal of Pressure Vessels and Piping*, 2009, 86(10): 711–718
 24. Nguyen-Thoi T, Liu G R, Vu-Do H C, Nguyen-Xuan H. An edge-based smoothed finite element method for visco-elastoplastic analyses of 2D solids using triangular mesh. *Computational Mechanics*, 2009, 45(1): 23–44
 25. Liu G R, Nguyen-Xuan H, Nguyen-Thoi T, Xu X. A novel Galerkin-like weakform and a superconvergent alpha finite element method (SaFEM) for mechanics problems using triangular meshes. *Journal of Computational Physics*, 2009, 228(11): 4055–4087
 26. Liu G R, Nguyen-Thoi T, Lam K Y. A novel FEM by scaling the gradient of strains with factor alpha (α FEM). *Computational Mechanics*, 2009, 43(3): 369–391
 27. Nguyen-Thoi T, Liu G R, Lam K Y, Zhang G Y. A face-based smoothed finite element method (FS-FEM) for 3D linear and geometrically non-linear solid mechanics problems using 4-node tetrahedral elements. *International Journal for Numerical Methods in Engineering*, 2009, 78(3): 324–353
 28. Nguyen-Thoi T, Liu G R, Vu-Do H C, Nguyen-Xuan H. A face-based smoothed finite element method (FS-FEM) for visco-elastoplastic analyses of 3D solids using tetrahedral mesh. *Computer Methods in Applied Mechanics and Engineering*, 2009, 198(41–44): 3479–3498
 29. He Z C, Liu G R, Zhong Z H, Cui X Y, Zhang G Y, Cheng A G. A coupled edge-/face-based smoothed finite element method for structural acoustic problems. *Applied Acoustics*, 2010, 71(10): 955–964
 30. Zhang Z Q, Yao J, Liu G R. An immersed smoothed finite element method for fluid-structure interaction problems. *International Journal of Computational Methods*, 2011, 8(4): 747–757
 31. Vu-Bac N, Nguyen-Xuan H, Chen L, Bordas S, Kerfriden P, Simpson R N, Liu G R, Rabczuk T. A node-based smoothed XFEM for fracture mechanics. *CMES: Comput Model Eng Sci*, 2011, 73: 331–356
 32. Chen L, Rabczuk T, Bordas S P A, Liu G R, Zeng K Y, Kerfriden P. Extended finite element method with edge-based strain smoothing (ESm-XFEM) for linear elastic crack growth. *Computer Methods in Applied Mechanics and Engineering*, 2012, 209–212: 250–265
 33. Nguyen-Xuan H, Liu G R. An edge-based smoothed finite element method softened with a bubble function (bES-FEM) for solid mechanics problems. *Computers & Structures*, 2013, 128: 14–30
 34. Zeng W, Liu G R, Kitamura Y, Nguyen-Xuan H. A three-dimensional ES-FEM for fracture mechanics problems in elastic solids. *Engineering Fracture Mechanics*, 2013, 114: 127–150
 35. Jiang C, Zhang Z Q, Liu G R, Han X, Zeng W. An edge-based/node-based selective smoothed finite element method using tetrahedrons for cardiovascular tissues. *Engineering Analysis with Boundary Elements*, 2015, 59: 62–77
 36. Zeng W, Liu G R, Li D, Dong X W. A smoothing technique based beta finite element method (β FEM) for crystal plasticity modeling. *Computers & Structures*, 2016, 162: 48–67
 37. Chen J S, Wu C T, Yoon S, You Y. A stabilized conforming nodal integration for Galerkin mesh-free methods. *International Journal for Numerical Methods in Engineering*, 2001, 50(2): 435–466
 38. Liu G R. On G space theory. *International Journal of Computational Methods*, 2009, 6(2): 257–289
 39. Liu G R, Nguyen-Thoi T, Nguyen-Xuan H, Dai K Y, Lam K Y. On the essence and the evaluation of the shape functions for the smoothed finite element method (SFEM) (Letter to Editor). *International Journal for Numerical Methods*, 2009, 77: 1863–1869
 40. Liu G R, Zhang G Y. A normed G space and weakened weak (W2) formulation of a cell-based smoothed point interpolation method. *International Journal of Computational Methods*, 2009, 6(1): 147–179
 41. Nguyen-Thoi T, Liu G R, Nguyen-Xuan H. Additional properties of the node-based smoothed finite element method (NS-FEM) for solid mechanics problems. *International Journal of Computational Methods*, 2009, 6(4): 633–666
 42. Nguyen-Thoi T. Development of Smoothed Finite Element Method (SFEM). Dissertation for the Doctoral Degree. Singapore: National University of Singapore, 2009
 43. Liu G R, Nguyen-Xuan H, Nguyen-Thoi T. A theoretical study on the smoothed FEM (S-FEM) models: properties, accuracy and convergence rates. *International Journal for Numerical Methods in Engineering*, 2010, 84(10): 1222–1256
 44. Liu G R. A G space theory and a weakened weak (W2) form for a

- unified formulation of compatible and incompatible methods: Part I theory. *International Journal for Numerical Methods in Engineering*, 2010, 81: 1093–1126
45. Liu G R. A G space theory and a weakened weak (W2) form for a unified formulation of compatible and incompatible methods: Part II applications to solid mechanics problems. *International Journal for Numerical Methods in Engineering*, 2010, 81: 1127–1156
 46. Nguyen-Xuan H, Nguyen H V, Bordas S, Rabczuk T, Duflo M. A cell-based smoothed finite element method for three dimensional solid structures. *KSCE Journal of Civil Engineering*, 2012, 16(7): 1230–1242
 47. He Z C, Li G Y, Zhong Z H, Cheng A G, Zhang G Y, Liu G R, Li E, Zhou Z. An edge-based smoothed tetrahedron finite element method (ES-T-FEM) for 3D static and dynamic problems. *Computational Mechanics*, 2013, 52(1): 221–236
 48. Nguyen-Thanh N, Rabczuk T, Nguyen-Xuan H, Bordas S P A. An alternative alpha finite element method (α FEM) for free and forced structural vibration using triangular meshes. *Journal of Computational and Applied Mathematics*, 2010, 233(9): 2112–2135
 49. Liu G R, Nguyen-Xuan H, Nguyen-Thoi T. A variationally consistent α FEM (VC α FEM) for solution bounds and nearly exact solution to solid mechanics problems using quadrilateral elements. *International Journal for Numerical Methods in Engineering*, 2011, 85(4): 461–497
 50. Cui X Y, Li G Y, Zheng G, Wu S Z. NS-FEM/ES-FEM for contact problems in metal forming analysis. *International Journal of Material Forming*, 2010, 3(S1): 887–890
 51. Li Y, Liu G R, Zhang G Y. An adaptive NS/ES-FEM approach for 2D contact problems using triangular elements. *Finite Elements in Analysis and Design*, 2011, 47(3): 256–275
 52. Xu X, Gu Y T, Liu G R. A hybrid smoothed finite element method (H-SFEM) to solid mechanics problems. *International Journal of Computational Methods*, 2013, 10(01): 1340011
 53. Zhao X, Bordas S P A, Qu J. A hybrid smoothed extended finite element/level set method for modeling equilibrium shapes of nano-inhomogeneities. *Computational Mechanics*, 2013, 52(6): 1417–1428
 54. Wu F, Liu G R, Li G Y, He Z C. A new hybrid smoothed FEM for static and free vibration analyses of Reissner-Mindlin Plates. *Computational Mechanics*, 2014, 54(3): 865–890
 55. Cui X Y, Chang S, Li G Y. A two-step Taylor Galerkin smoothed finite element method for Lagrangian dynamic problem. *International Journal of Computational Methods*, 2015, 12(04): 1540004
 56. Li E, He Z C, Xu X, Liu G R, Gu Y T. A three-dimensional hybrid smoothed finite element method (H-SFEM) for nonlinear solid mechanics problems. *Acta Mechanica*, 2015, 226(12): 4223–4245
 57. Lee K, Son Y, Im S. Three-dimensional variable-node elements based upon CS-FEM for elastic-plastic analysis. *Computers & Structures*, 2015, 158: 308–332
 58. Li Y, Zhang G Y, Liu G R, Huang Y N, Zong Z. A contact analysis approach based on linear complementarity formulation using smoothed finite element methods. *Engineering Analysis with Boundary Elements*, 2013, 37(10): 1244–1258
 59. Cui X Y, Li G Y. Metal forming analysis using the edge-based smoothed finite element method. *Finite Elements in Analysis and Design*, 2013, 63: 33–41
 60. Zeng W, Larsen J M, Liu G R. Smoothing technique based crystal plasticity finite element modeling of crystalline materials. *International Journal of Plasticity*, 2015, 65: 250–268
 61. Cui X Y, Liu G R, Li G Y, Zhang G Y, Zheng G. Analysis of plates and shells using an edge-based smoothed finite element method. *Computational Mechanics*, 2010, 45(2–3): 141–156
 62. Nguyen-Xuan H, Liu G R, Thai-Hoang C, Nguyen-Thoi T. An edge-based smoothed finite element method (ES-FEM) with stabilized discrete shear gap technique for analysis of Reissner-Mindlin plates. *Computer Methods in Applied Mechanics and Engineering*, 2010, 199(9–12): 471–489
 63. Zhang Z Q, Liu G R. An edge-based smoothed finite element method (ES-FEM) using 3-node triangular elements for 3D non-linear analysis of spatial membrane structures. *International Journal for Numerical Methods*, 2011, 86(2): 135–154
 64. Baiz P M, Natarajan S, Bordas S P A, Kerfriden P, Rabczuk T. Linear buckling analysis of cracked plates by SFEM and XFEM. *Journal of Mechanics of Materials and Structures*, 2011, 6(9–10): 1213–1238
 65. Zheng G, Cui X, Li G, Wu S. An edge-based smoothed triangle element for non-linear explicit dynamic analysis of shells. *Computational Mechanics*, 2011, 48(1): 65–80
 66. Wu C T, Wang H P. An enhanced cell-based smoothed finite element method for the analysis of Reissner-Mindlin plate bending problems involving distorted mesh. *International Journal for Numerical Methods in Engineering*, 2013, 95(4): 288–312
 67. Nguyen-Thoi T, Bui-Xuan T, Phung-Van P, Nguyen-Hoang S, Nguyen-Xuan H. An edge-based smoothed three-node Mindlin plate element (ES-MIN3) for static and free vibration analyses of plates. *KSCE Journal of Civil Engineering*, 2014, 18(4): 1072–1082
 68. Luong-Van H, Nguyen-Thoi T, Liu G R, Phung-Van P. A cell-based smoothed finite element method using three-node shear-locking free Mindlin plate element (CS-FEM-MIN3) for dynamic response of laminated composite plates on viscoelastic foundation. *Engineering Analysis with Boundary Elements*, 2014, 42: 8–19
 69. Élie-Dit-Cosaque X J, Gakwaya A, Naceur H. Smoothed finite element method implemented in a resultant eight-node solid-shell element for geometrical linear analysis. *Computational Mechanics*, 2015, 55(1): 105–126
 70. Phung-Van P, Nguyen-Thoi T, Bui-Xuan T, Lieu-Xuan Q. A cell-based smoothed three-node Mindlin plate element (CS-FEM-MIN3) based on the C 0-type higher-order shear deformation for geometrically nonlinear analysis of laminated composite plates. *Computational Materials Science*, 2015, 96: 549–558
 71. Nguyen-Thoi T, Rabczuk T, Ho-Huu V, Le-Anh L, Dang-Trung H, Vo-Duy T. An extended cell-based smoothed three-node Mindlin plate element (XCS-MIN3) for free vibration analysis of cracked FGM plates. *International Journal of Computational Methods*, 2016, 2016: 1750011
 72. Cui X Y, Liu G R, Li G Y. Bending and vibration responses of laminated composite plates using an edge-based smoothing technique. *Engineering Analysis with Boundary Elements*, 2011, 35(6): 818–826
 73. Herath M T, Natarajan S, Prusty B G, John N S. Smoothed finite

- element and genetic algorithm based optimization for shape adaptive composite marine propellers. *Composite Structures*, 2014, 109: 189–197
74. Li E, Zhang Z, Chang C C, Liu G R, Li Q. Numerical homogenization for incompressible materials using selective smoothed finite element method. *Composite Structures*, 2015, 123: 216–232
 75. Tran T N, Liu G R, Nguyen-Xuan H, Nguyen-Thoi T. An edge-based smoothed finite element method for primal-dual shakedown analysis of structures. *International Journal for Numerical Methods in Engineering*, 2010, 82(7): 917–938
 76. Nguyen-Xuan H, Rabczuk T. Adaptive selective ES-FEM limit analysis of cracked plane-strain structures. *Frontiers of Structural and Civil Engineering*, 2015, 9(4): 478–490
 77. Chen L, Liu G R, Nourbakhsh N, Zeng K. A singular edge-based smoothed finite element method (ES-FEM) for bimaterial interface cracks. *Computational Mechanics*, 2010, 45(2–3): 109–125
 78. Liu G R, Chen L, Nguyen T-Thoi K, Zeng G Y, Zhang. A novel singular node-based smoothed finite element method (NS-FEM) for upper bound solutions of fracture problems. *International Journal for Numerical Methods in Engineering*, 2010, 83(11): 1466–1497
 79. Liu G R, Nourbakhshnia N, Chen L, Zhang Y W. A novel general formulation for singular stress field using the ES-FEM method for the analysis of mixed-mode cracks. *International Journal of Computational Methods*, 2010, 7(1): 191–214
 80. Liu G R, Nourbakhshnia N, Zhang Y W. A novel singular ES-FEM method for simulating singular stress fields near the crack tips for linear fracture problems. *Engineering Fracture Mechanics*, 2011, 78(6): 863–876
 81. Nourbakhshnia N, Liu G R. A quasi-static crack growth simulation based on the singular ES-FEM. *International Journal for Numerical Methods in Engineering*, 2011, 88(5): 473–492
 82. Chen L, Liu G R, Jiang Y, Zeng K, Zhang J. A singular edge-based smoothed finite element method (ES-FEM) for crack analyses in anisotropic media. *Engineering Fracture Mechanics*, 2011, 78(1): 85–109
 83. Jiang Y, Liu G R, Zhang Y W, Chen L, Tay T E. A singular ES-FEM for plastic fracture mechanics. *Computer Methods in Applied Mechanics and Engineering*, 2011, 200(45–46): 2943–2955
 84. Chen L, Liu G R, Zeng K, Zhang J. A novel variable power singular element in G space with strain smoothing for bi-material fracture analyses. *Engineering Analysis with Boundary Elements*, 2011, 35(12): 1303–1317
 85. Chen L, Liu G R, Zeng K. A combined extended and edge-based smoothed finite element method (ES-XFEM) for fracture analysis of 2D elasticity. *International Journal of Computational Methods*, 2011, 8(4): 773–786
 86. Nourbakhshnia N, Liu G R. Fatigue analysis using the singular ES-FEM. *International Journal of Fatigue*, 2012, 40: 105–111
 87. Nguyen-Xuan H, Liu G R, Nourbakhshnia N, Chen L. A novel singular ES-FEM for crack growth simulation. *Engineering Fracture Mechanics*, 2012, 84: 41–66
 88. Liu P, Bui T Q, Zhang C, Yu T T, Liu G R, Golub M V. The singular edge-based smoothed finite element method for stationary dynamic crack problems in 2D elastic solids. *Computer Methods in Applied Mechanics and Engineering*, 2012, 233–236: 68–80
 89. Jiang Y, Tay T E, Chen L, Sun X S. An edge-based smoothed XFEM for fracture in composite materials. *International Journal of Fracture*, 2013, 179(1–2): 179–199
 90. Nguyen-Xuan H, Liu G R, Bordas S, Natarajan S, Rabczuk T. An adaptive singular ES-FEM for mechanics problems with singular field of arbitrary order. *Computer Methods in Applied Mechanics and Engineering*, 2013, 253: 252–273
 91. Vu-Bac N, Nguyen-Xuan H, Chen L, Lee C K, Zi G, Zhuang X, Liu G R, Rabczuk T. A phantom-node method with edge-based strain smoothing for linear elastic fracture mechanics. *Journal of Applied Mathematics*, 2013, 2013: 1
 92. Liu G R, Chen L, Li M. S-FEM for fracture problems, theory, formulation and application. *International Journal of Computational Methods*, 2014, 11(03): 1343003
 93. Jiki P N, Agber J U. Damage evaluation in gap tubular truss ‘K’ bridge joints using SFEM. *Journal of Constructional Steel Research*, 2014, 93: 135–142
 94. Jiang Y, Tay T E, Chen L, Zhang Y W. Extended finite element method coupled with face-based strain smoothing technique for three-dimensional fracture problems. *International Journal for Numerical Methods in Engineering*, 2015, 102(13): 1894–1916
 95. Zeng W, Liu G R, Jiang C, Dong X W, Chen H D, Bao Y, Jiang Y. An effective fracture analysis method based on the virtual crack closure-integral technique implemented in CS-FEM. *Applied Mathematical Modelling*, 2016, 40(5–6): 3783–3800
 96. Chen H, Wang Q, Liu G R, Wang Y, Sun J. Simulation of thermoelastic crack problems using singular edge-based smoothed finite element method. *International Journal of Mechanical Sciences*, 2016, 115–116: 123–134
 97. Wu L, Liu P, Shi C, Zhang Z, Bui T Q, Jiao D. Edge-based smoothed extended finite element method for dynamic fracture analysis. *Applied Mathematical Modelling*, 2016, 40(19–20): 8564–8579
 98. Liu G R, Zeng W, Nguyen-Xuan H. Generalized stochastic cell-based smoothed finite element method (GS_CS-FEM) for solid mechanics. *Finite Elements in Analysis and Design*, 2013, 63: 51–61
 99. Hu X B, Cui X Y, Feng H, Li G Y. Stochastic analysis using the generalized perturbation stable node-based smoothed finite element method. *Engineering Analysis with Boundary Elements*, 2016, 70: 40–55
 100. Zhang Z Q, Liu G R. Temporal stabilization of the node-based smoothed finite element method and solution bound of linear elastostatics and vibration problems. *Computational Mechanics*, 2010, 46(2): 229–246
 101. Zhang Z Q, Liu G R. Upper and lower bounds for natural frequencies: a property of the smoothed finite element methods. *International Journal for Numerical Methods in Engineering*, 2010, 84(2): 149–178
 102. Wang L, Han D, Liu G R, Cui X. Free vibration analysis of double-walled carbon nanotubes using the smoothed finite element method. *International Journal of Computational Methods*, 2011, 8(4): 879–890
 103. He Z, Li G, Zhong Z, Cheng A, Zhang G, Li E. An improved modal analysis for three-dimensional problems using face-based

- smoothed finite element method. *Acta Mechanica Solida Sinica*, 2013, 26(2): 140–150
104. Cui X Y, Li G Y, Liu G R. An explicit smoothed finite element method (SFEM) for elastic dynamic problems. *International Journal of Computational Methods*, 2013, 10(1): 1340002
 105. Nguyen-Thoi T, Phung-Van P, Rabczuk T, Nguyen-Xuan H, Le-Van C. Free and forced vibration analysis using the n-sided polygonal cell-based smoothed finite element method (n CS-FEM). *International Journal of Computational Methods*, 2013, 10(1): 1340008
 106. Feng H, Cui X Y, Li G Y, Feng S Z. A temporal stable node-based smoothed finite element method for three-dimensional elasticity problems. *Computational Mechanics*, 2014, 53(5): 859–876
 107. Yang G, Hu D, Ma G, Wan D. A novel integration scheme for solution of consistent mass matrix in free and forced vibration analysis. *Meccanica*, 2016, 51(8): 1897–1911
 108. Cui X Y, Hu X, Li G Y, Liu G R. A modified smoothed finite element method for static and free vibration analysis of solid mechanics. *International Journal of Computational Methods*, 2016, 13(6), 1650043
 109. He Z C, Liu G R, Zhong Z H, Zhang G Y, Cheng A G. Dispersion free analysis of acoustic problems using the alpha finite element method. *Computational Mechanics*, 2010, 46(6): 867–881
 110. He Z C, Liu G R, Zhong Z H, Zhang G Y, Cheng A G. Coupled analysis of 3D structural-acoustic problems using the edge-based smoothed finite element method/finite element method. *Finite Elements in Analysis and Design*, 2010, 46(12): 1114–1121
 111. Yao L Y, Yu D J, Cui X Y, Zang X G. Numerical treatment of acoustic problems with the smoothed finite element method. *Applied Acoustics*, 2010, 71(8): 743–753
 112. He Z C, Cheng A G, Zhang G Y, Zhong Z H, Liu G R. Dispersion error reduction for acoustic problems using the edge - based smoothed finite element method (ES-FEM). *International Journal for Numerical Methods in Engineering*, 2011, 86(11): 1322–1338
 113. He Z C, Li G Y, Zhong Z H, Cheng A G, Zhang G Y, Li E, Liu G R. An ES-FEM for accurate analysis of 3D mid-frequency acoustics using tetrahedron mesh. *Computers & Structures*, 2012, 106–107: 125–134
 114. Li W, Chai Y, Lei M, Liu G R. Analysis of coupled structural-acoustic problems based on the smoothed finite element method (S-FEM). *Engineering Analysis with Boundary Elements*, 2014, 42: 84–91
 115. Li E, He Z C, Xu X, Liu G R. Hybrid smoothed finite element method for acoustic problems. *Computer Methods in Applied Mechanics and Engineering*, 2015, 283: 664–688
 116. He Z C, Li G Y, Liu G R, Cheng A G, Li E. Numerical investigation of ES-FEM with various mass re-distribution for acoustic problems. *Applied Acoustics*, 2015, 89: 222–233
 117. Wu F, Liu G R, Li G Y, Cheng A G, He Z C, Hu Z H. A novel hybrid FS-FEM/SEA for the analysis of vibro-acoustic problems. *International Journal for Numerical Methods in Engineering*, 2015, 102(12): 1815–1829
 118. He Z, Li G, Zhang G, Liu G R, Gu Y, Li E. Acoustic analysis using a mass-redistributed smoothed finite element method with quadrilateral mesh. *Engineering Computation*, 2015, 32(8): 2292–2317
 119. He Z C, Li E, Li G Y, Wu F, Liu G R, Nie X. Acoustic simulation using α -FEM with a general approach for reducing dispersion error. *Engineering Analysis with Boundary Elements*, 2015, 61: 241–253
 120. Wang G, Cui X Y, Feng H, Li G Y. A stable node-based smoothed finite element method for acoustic problems. *Computer Methods in Applied Mechanics and Engineering*, 2015, 297: 348–370
 121. Wang G, Cui X Y, Liang Z M, Li G Y. A coupled smoothed finite element method (S-FEM) for structural-acoustic analysis of shells. *Engineering Analysis with Boundary Elements*, 2015, 61: 207–217
 122. Chai Y, Li W, Gong Z, Li T. Hybrid smoothed finite element method for two-dimensional underwater acoustic scattering problems. *Ocean Engineering*, 2016, 116: 129–141
 123. Chai Y, Li W, Gong Z, Li T. Hybrid smoothed finite element method for two dimensional acoustic radiation problems. *Appl Acoust.*, 2016, 103: 90–101
 124. Wu F, He Z C, Liu G R, Li G Y, Cheng A G. A novel hybrid ES-FE-SEA for mid-frequency prediction of Transmission losses in complex acoustic systems. *Applied Acoustics*, 2016, 111: 198–204
 125. Kumar V, Metha R. Impact simulations using smoothed finite element method. *International Journal of Computational Methods*, 2013, 10(4): 1350012
 126. Nguyen-Thoi T, Liu G R, Nguyen-Xuan H, Nguyen-Tran C. Adaptive analysis using the node-based smoothed finite element method (NS-FEM). *International Journal for Numerical Methods in Biomedical Engineering*, 2011, 27(2): 198–218
 127. Nguyen-Xuan H, Wu C T, Liu G R. An adaptive selective ES-FEM for plastic collapse analysis. *European Journal of Mechanics-A/ Solids*, 2016, 58: 278–290
 128. Kazemzadeh-Parsi M J, Daneshmand F. Solution of geometric inverse heat conduction problems by smoothed fixed grid finite element method. *Finite Elements in Analysis and Design*, 2009, 45 (10): 599–611
 129. Li E, Liu G R, Tan V. Simulation of hyperthermia treatment using the edge-based smoothed finite-element method. *Numerical Heat Transfer*, 2010, 57(11): 822–847
 130. Li E, Liu G R, Tan V, He Z C. An efficient algorithm for phase change problem in tumor treatment using α FEM. *International Journal of Thermal Sciences*, 2010, 49(10): 1954–1967
 131. Kumar V. Smoothed finite element methods for thermo-mechanical impact problems. *International Journal of Computational Methods*, 2013, 10(1): 1340010
 132. Xue B Y, Wu S C, Zhang W H, Liu G R. A smoothed FEM (S-FEM) for heat transfer problems. *International Journal of Computational Methods*, 2013, 10(1): 1340001
 133. Feng S Z, Cui X Y, Li G Y. Analysis of transient thermo-elastic problems using edge-based smoothed finite element method. *International Journal of Thermal Sciences*, 2013, 65: 127–135
 134. Feng S Z, Cui X Y, Li G Y, Feng H, Xu F X. Thermo-mechanical analysis of functionally graded cylindrical vessels using edge-based smoothed finite element method. *International Journal of Pressure Vessels and Piping*, 2013, 111–112: 302–309
 135. Feng S Z, Cui X Y, Li G Y. Transient thermal mechanical analyses using a face-based smoothed finite element method (FS-FEM). *International Journal of Thermal Sciences*, 2013, 74: 95–103
 136. Li E, He Z C, Xu X. An edge-based smoothed tetrahedron finite element method (ES-T-FEM) for thermomechanical problems. *International Journal of Heat and Mass Transfer*, 2013, 66: 723–

732

137. Feng S, Cui X, Li G. Thermo-mechanical analyses of composite structures using face-based smoothed finite element method. *International Journal of Applied Mechanics*, 2014, 6(2): 1450020
138. Li E, Zhang Z, He Z C, Xu X, Liu G R, Li Q. Smoothed finite element method with exact solutions in heat transfer problems. *International Journal of Heat and Mass Transfer*, 2014, 78: 1219–1231
139. Feng S, Cui X, Li G. Thermo-mechanical analysis of composite pressure vessels using edge-based smoothed finite element method. *International Journal of Computational Methods*, 2014, 11(6): 1350089
140. Cui X Y, Li Z C, Feng H, Feng S Z. Steady and transient heat transfer analysis using a stable node-based smoothed finite element method. *International Journal of Thermal Sciences*, 2016, 110: 12–25
141. Nguyen-Xuan H, Liu G R, Nguyen-Thoi T, Nguyen-Tran C. An edge-based smoothed finite element method for analysis of two-dimensional piezoelectric structures. *Smart Materials and Structures*, 2009, 18(6): 065015
142. Olyae M S, Razfar M R, Kansa E J. Reliability based topology optimization of a linear piezoelectric micromotor using the cell-based smoothed finite element method. *Computer Modeling in Engineering & Sciences*, 2011, 75(1): 43–87
143. Olyae M S, Razfar M R, Wang S, Kansa E J. Topology optimization of a linear piezoelectric micromotor using the smoothed finite element method. *Computer Modeling in Engineering & Sciences*, 2011, 82(1): 55–81
144. Chen L, Zhang Y W, Liu G R, Nguyen-Xuan H, Zhang Z Q. A stabilized finite element method for certified solution with bounds in static and frequency analyses of piezoelectric structures. *Computer Methods in Applied Mechanics and Engineering*, 2012, 241–244: 65–81
145. Li E, He Z C, Chen L, Li B, Xu X, Liu G R. An ultra-accurate hybrid smoothed finite element method for piezoelectric problem. *Engineering Analysis with Boundary Elements*, 2015, 50: 188–197
146. Atia K S R, Heikal A M, Obayya S S A. Efficient smoothed finite element time domain analysis for photonic devices. *Optics Express*, 2015, 23(17): 22199–22213
147. He Z C, Liu G R, Zhong Z H, Zhang G Y, Cheng A G. A coupled ES-FEM/BEM method for fluid-structure interaction problems. *Engineering Analysis with Boundary Elements*, 2011, 35(1): 140–147
148. Zhang Z Q, Liu G R, Khoo B C. Immersed smoothed finite element method for two dimensional fluid-structure interaction problems. *International Journal for Numerical Methods in Engineering*, 2012, 90(10): 1292–1320
149. Yao J, Liu G R, Narmoneva D A, Hinton R B, Zhang Z Q. Immersed smoothed finite element method for fluid-structure interaction simulation of aortic valves. *Computational Mechanics*, 2012, 50(6): 789–804
150. Zhang Z Q, Liu G R, Khoo B C. A three dimensional immersed smoothed finite element method (3D IS-FEM) for fluid-structure interaction problems. *Computational Mechanics*, 2013, 51(2): 129–150
151. Nguyen-Thoi T, Phung-Van P, Rabczuk T, Nguyen-Xuan H, Le-Van C. An application of the ES-FEM in solid domain for dynamic analysis of 2D fluid-solid interaction problems. *International Journal of Computational Methods*, 2013, 10(1): 1340003
152. Wang S, Khoo B C, Liu G R, Xu G X, Chen L. Coupling GSM/ALE with ES-FEM-T3 for fluid-deformable structure interactions. *Journal of Computational Physics*, 2014, 276: 315–340
153. Nguyen-Thoi T, Phung-Van P, Nguyen-Hoang S, Lieu-Xuan Q (2014) A smoothed coupled NS/nES-FEM for dynamic analysis of 2D fluid-solid interaction problems.
154. He T. On a partitioned strong coupling algorithm for modeling fluid-structure interaction. *International Journal of Applied Mechanics*, 2015, 7(2): 1550021
155. He T. Semi-implicit coupling of CS-FEM and FEM for the interaction between a geometrically nonlinear solid and an incompressible fluid. *International Journal of Computational Methods*, 2015, 12(5): 1550025
156. Zhang Z Q, Liu G R. Solution bound and nearly exact solution to nonlinear solid mechanics problems based on the smoothed FEM concept. *Engineering Analysis with Boundary Elements*, 2014, 42: 99–114
157. Jiang C, Zhang Z Q, Han X, Liu G R. Selective smoothed finite element methods for extremely large deformation of anisotropic incompressible bio-tissues. *International Journal for Numerical Methods in Engineering*, 2014, 99(8): 587–610
158. Onishi Y, Amaya K. A locking-free selective smoothed finite element method using tetrahedral and triangular elements with adaptive mesh rezoning for large deformation problems. *International Journal for Numerical Methods in Engineering*, 2014, 99(5): 354–371
159. Jiang C, Liu G R, Han X, Zhang Z Q, Zeng W. A smoothed finite element method for analysis of anisotropic large deformation of passive rabbit ventricles in diastole. *International Journal for Numerical Methods in Biomedical Engineering*, 2015, 31(1): 1–25
160. Onishi Y, Iida R, Amaya K. F-bar aided edge-based smoothed finite element method using tetrahedral elements for finite deformation analysis of nearly incompressible solids. *International Journal for Numerical Methods in Engineering*, 2015, 109: 771–773
161. Li E, Chen J, Zhang Z, Fang J, Liu G R, Li Q. Smoothed finite element method for analysis of multi-layered systems - Applications in biomaterials. *Computers & Structures*, 2016, 168: 16–29
162. Li E, Liao W H. An efficient finite element algorithm in elastography. *International Journal of Applied Mechanics*, 2016, 8(3): 1650037
163. Niu R P, Liu G R, Yue J H. Development of a software package of smoothed finite element method (S-FEM) for solid mechanics problems. *International Journal of Computational Methods*, 2018, 15(3): 1845004
164. Jiang C, Han X, Zhang Z Q, Liu G R, Gao G J. A locking-free face-based S-FEM via averaging nodal pressure using 4-nodes tetrahedrons for 3D explicit dynamics and quasi-statics. *International Journal of Computational Methods*, 2018, 15(6): 1850043
165. Yue J, Liu G R, Li M, Niu R. A cell-based smoothed finite element method for multi-body contact analysis using linear complementarity formulation. *International Journal of Solids and Structures*, 2018, 141–142: 110–126

166. Du C F, Zhang D G, Li L, Liu G R. A node-based smoothed point interpolation method for dynamic analysis of rotating flexible beams. *Chinese Journal of Theoretical and Applied Mechanics*, 2018, 34(2): 409–420
167. Zeng W, Liu G R. Smoothed finite element methods (S-FEM): an overview and recent developments. *Archives of Computational Methods in Engineering*, 2018, 25(2): 397–435
168. Li Y H, Li M, Liu G R. A novel alpha smoothed finite element method for ultra-accurate solution using quadrilateral elements. *International Journal of Computational Methods*, 2018, 15(3): 1845008
169. Rong X, Niu R, Liu G. Stability analysis of smoothed finite element methods with explicit method for transient heat transfer problems. *International Journal of Computational Methods*, 2018, 15(3): 1845005
170. Zhang J F, Niu R P, Zhang Y F, Wang C Q, Li M, Liu G R. Development of SFEM-Pre: a novel preprocessor for model creation for the smoothed finite element method. *International Journal of Computational Methods*, 2018, 15(1): 1845002
171. Jiang C, Zhang Z Q, Han X, Liu G, Lin T. A cell-based smoothed finite element method with semi-implicit CBS procedures for incompressible laminar viscous flows. *International Journal for Numerical Methods in Fluids*, 2018, 86(1): 20–45
172. Wu F, Zeng W, Yao L Y, Liu G R. A generalized probabilistic edge-based smoothed finite element method for elastostatic analysis of Reissner-Mindlin plates. *Applied Mathematical Modelling*, 2018, 53: 333–352
173. Nguyen-Thoi T, Bui-Xuan T, Liu G R, Vo-Duy T. Static and free vibration analysis of stiffened flat shells by a cell-based smoothed discrete shear gap method (CS-FEM-DSG3) using three-node triangular elements. *International Journal of Computational Methods*, 2018, 15(6): 1850056
174. Bhowmick S, Liu G R. On singular ES-FEM for fracture analysis of solids with singular stress fields of arbitrary order. *Engineering Analysis with Boundary Elements*, 2018, 86: 64–81
175. Jiang C, Han X, Liu G R, Zhang Z Q, Yang G, Gao G J. Smoothed finite element methods (S-FEMs) with polynomial pressure projection (P3) for incompressible solids. *Engineering Analysis with Boundary Elements*, 2017, 84: 253–269
176. Liu G R, Chen M, Li M. Lower bound of vibration modes using the node-based smoothed finite element method (NS-FEM). *International Journal of Computational Methods*, 2017, 14(4): 1750036
177. Du C F, Zhang D G, Liu G R. A cell-based smoothed finite element method for free vibration analysis of a rotating plate. *International Journal of Computational Methods*, 2017, 14(5): 1840003
178. Chai Y, Li W, Liu G R, Gong Z, Li T. A superconvergent alpha finite element method (α FEM) for static and free vibration analysis of shell structures. *Computers & Structures*, 2017, 179: 27–47
179. Li Y, Yue J H, Niu R P, Liu G R. Automatic mesh generation for 3D smoothed finite element method (S-FEM) based on the weaken-weak formulation. *Advances in Engineering Software*, 2016, 99: 111–120
180. Yue J H, Li M, Liu G R, Niu R P. Proofs of the stability and convergence of a weakened weak method using PIM shape functions. *Computers & Mathematics with Applications*, 2016, 72(4): 933–951
181. Chen M, Li M, Liu G R. Mathematical basis of g spaces. *International Journal of Computational Methods*, 2016, 13(4): 1641007
182. Tootoonchi A, Khoshghalb A, Liu G R, Khalili N. A cell-based smoothed point interpolation method for flow-deformation analysis of saturated porous media. *Computers and Geotechnics*, 2016, 75: 159–173
183. Liu G R. On partitions of unity property of nodal shape functions: rigid-body-movement reproduction and mass conservation. *International Journal of Computational Methods*, 2016, 13(02): 1640003
184. He Z C, Zhang G Y, Deng L, Li E, Liu G R. Topology optimization using node-based smoothed finite element method. *International Journal of Applied Mechanics*, 2015, 7(06): 1550085
185. Nguyen-Xuan H, Liu G R. An edge-based finite element method (ES-FEM) with adaptive scaled-bubble functions for plane strain limit analysis. *Computer Methods in Applied Mechanics and Engineering*, 2015, 285: 877–905
186. Wu C T, Hu W, Liu G R. Bubble-enhanced smoothed finite element formulation: a variational multi-scale approach for volume-constrained problems in two-dimensional linear elasticity. *International Journal for Numerical Methods in Engineering*, 2014, 100(5): 374–398
187. Jiang C, Zhang Z Q, Han X, Liu G R. Selective smoothed finite element methods for extremely large deformation of anisotropic incompressible bio-tissues. *International Journal for Numerical Methods in Engineering*, 2014, 99(8): 587–610
188. Wu F, Liu G R, Li G Y, Liu Y J, He Z C. A coupled ES-BEM and FM-BEM for structural acoustic problems. *Noise Control Engineering Journal*, 2014, 62(4): 196–209
189. Hu D, Wang Y, Liu G R, Li T, Han X, Gu Y T. A sub-domain smoothed Galerkin method for solid mechanics problems. *International Journal for Numerical Methods in Engineering*, 2014, 98(11): 781–798
190. Li Y, Li M, Liu G R. A modified triangulation algorithm tailored for the smoothed finite element method (S-FEM). *International Journal of Computational Methods*, 2014, 11(01): 1350069
191. Timoshenko S P, Goodier J N. *Theory of Elasticity*. 3rd ed. New York: McGraw-Hill, 1970
192. T-Thoi Nguyen, Liu G R, Nguyen-Xuan H. An n-sided polygonal edge-based smoothed finite element method (n ES-FEM) for solid mechanics. *International Journal for Numerical Methods in Biomedical Engineering*, 2011, 27(9): 1446–1472
193. Wang S. An ABAQUS implementation of the cell-based smoothed finite element method using quadrilateral elements. Thesis for the Master's Degree. Cincinnati: University of Cincinnati, 2014
194. Liu G R, Li Y, Dai K Y, Luan M T, Xue W. A linearly conforming radial point interpolation method for solid mechanics problems. *International Journal of Computational Methods*, 2006, 3(4): 401–428
195. Ong T H, Heaney C E, Lee C K, Liu G R, Nguyen-Xuan H. On stability, convergence and accuracy of bES-FEM and bFS-FEM for nearly incompressible elasticity. *Computer Methods in Applied Mechanics and Engineering*, 2015, 285: 315–345
196. Wu C T, Hu W, Liu G R. Bubble-enhanced smoothed finite

- element formulation: a variational multi-scale approach for volume-constrained problems in two-dimensional linear elasticity. *International Journal for Numerical Methods in Engineering*, 2014, 100(5): 374–398
197. Leonetti L, Garcea G, Nguyen-Xuan H. A mixed edge-based smoothed finite element method (MES-FEM) for elasticity. *Computers & Structures*, 2016, 173: 123–138
198. Zeng W, Liu G R, Jiang C, Nguyen-Thoi T, Jiang Y. A generalized beta finite element method with coupled smoothing techniques for solid mechanics. *Engineering Analysis with Boundary Elements*, 2016, 73: 103–119
199. Liu G R. On partitions of unity property of nodal shape functions: rigid-body-movement reproduction and mass conservation. *International Journal of Computational Methods*, 2016, 13(2): 1640003
200. Yue J H, Li M, Liu G R, Niu R P. Proofs of the stability and convergence of a weakened weak method using PIM shape functions. *Computers & Mathematics with Applications*, 2016, 72 (4): 933–951
201. Liu G R, Zhang G Y, Wang Y Y, Zhong Z H, Li G Y, Han X. A nodal integration technique for meshfree radial point interpolation method (NI-RPCM). *International Journal of Solids and Structures*, 2007, 44(11–12): 3840–3860
202. Liu G R, Liu M B. *Smoothed Particle Hydrodynamics: A Meshfree Particle Method*. Singapore: World Scientific, 2003
203. Liu M B, Liu G R. Smoothed particle hydrodynamics (SPH): an overview and recent developments. *Archives of Computational Methods in Engineering*, 2010, 17(1): 25–76
204. Liu M B, Liu G R, Zhou L W, Chang J Z. Dissipative particle dynamics (DPD): an overview and recent developments. *Archives of Computational Methods in Engineering*, 2015, 17(1): 25–76
205. Liu J, Zhang Z Q, Zhang G Y. A smoothed finite element method (S-FEM) for large-deformation elastoplastic analysis. *International Journal of Computational Methods*, 2015, 12(4): 1–26
206. Li E, Zhang Z, Chang C C, Zhou S, Liu G R, Li Q. A new homogenization formulation for multifunctional composites. *International Journal of Computational Methods*, 2016, 13(2): 1640002
207. Liu G R, Han X, Xu Y G, Lam K Y. Material characterization of functionally graded material using elastic waves and a progressive learning neural network. *Composites Science and Technology*, 2001, 61(10): 1401–1411
208. Liu G R, Han X, Lam K Y. Determination of elastic constants of anisotropic laminated plates using elastic waves and a progressive neural network. *Journal of Sound and Vibration*, 2002, 252(2): 239–259
209. Liu G R, Han X. *Computational inverse techniques in nondestructive evaluation*. CRC Press, 2003
210. Li Y, Liu G R. An element-free smoothed radial point interpolation method (EFS-RPIM) for 2D and 3D solid mechanics problems. *Computers and Mathematics with Applications*, 2018, doi: 10.1016/j.camwa.2018.09.047
211. Liu G R. A novel pick-out theory and technique for constructing the smoothed derivatives of functions for numerical methods. *International Journal of Computational Methods*, 2018, 15(3): 1850070